



**The repurposing of ivermectin for malaria: a prospective pharmacokinetics-based virtual clinical trials assessment of dosing regimen options**

Journal:	<i>Journal of Pharmaceutical Sciences</i>
Manuscript ID	18-018.R1
Article Type:	Research Article
Date Submitted by the Author:	n/a
Complete List of Authors:	Badhan, Raj; Aston University, School of Pharmacy, Life & Health Sciences Zakaria, Zamil; Aston University, School of Pharmacy, Life & Health Sciences; Ministry Of Health Malaysia, , Block E1, E3, E6, E7 & E10, Parcel E, Federal Government Administration Centre Olafuyi, Olusola; Aston University, School of Pharmacy, Life & Health Sciences
Keywords:	Physiologically based pharmacokinetic modeling, Pharmacokinetics, Drug resistance, Onychomycosis, In silico modeling

**The repurposing of ivermectin for malaria: a prospective pharmacokinetics-based virtual clinical trials assessment of dosing regimen options**

**Raj Badhan<sup>1</sup>, Zaril Zakaria<sup>2,3</sup> and Olusola Olafuyi<sup>3</sup>**

<sup>1</sup> Applied Health Research Group, Aston Pharmacy School, Aston University, Birmingham, B4 7ET, United Kingdom.

<sup>2</sup> Ministry Of Health Malaysia, Block E1, E3, E6, E7 & E10, Parcel E, Federal Government Administration Centre, 62590, Putrajaya, Malaysia

<sup>3</sup> Aston Pharmacy School, Aston University, Birmingham, B4 7ET, United Kingdom.

**Correspondence:**

Dr Raj Badhan  
Aston Pharmacy School  
Life and Health Sciences  
Aston University  
Birmingham  
B4 7ET  
UK  
Telephone: +44 121 204 3288  
E-mail: r.k.s.badhan@aston.ac.uk

**ABSTRACT**

Ivermectin has demonstrated many successes in the treatment of a range of nematode infections. Considering the increase in malaria resistance attention has turned towards ivermectin as a candidate for repurposing for malaria. This study developed and validated an ivermectin physiologically-based pharmacokinetic model in healthy adults (20-50 years) and paediatric (3-5 years/15-25 kg) subjects and in a representative adult malaria population group (Thailand). Dosing optimisation demonstrated a twice daily for 3- or 5-day regimens would provide a time above the LC50 of more than 7 days for adult and paediatric. Furthermore, to address the occurrence of CYP450-induction often encountered with antiretroviral agents, simulated drug-drug interaction studies with efavirenz highlighted that a 1 mg/kg once daily dose for five days would counteract the increased ivermectin hepatic clearance and enable a time above LC50 of 138.8 hours in adults and 141.2 hours in paediatric subjects.

It was also demonstrated that dosage regimen design would require consideration of the age-weight geographical relationship of the subjects, with a dosage regimen for a representative Thailand population group requiring at least a single daily dose for 5 days to maintain ivermectin plasma concentrations and a time above LC50 similar to that in healthy adults.

**KEYWORDS**

Physiologically-based pharmacokinetics; pharmacokinetics; drug resistance; Onychomycosis;  
*in-silico* modelling.

For Peer Review

## 1. INTRODUCTION

In May 2015, the World Health Organisation published a future strategy for tackling malaria, the 'Global Technical Strategy for Malaria 2016-2030'<sup>1</sup>, which highlighted the need for continued work towards tackling the significant risks many of the world's population face with malaria infection. It has been estimated that 3.2 billion people are at risk of malaria with up to 283 million cases of diagnosed malaria worldwide in 2013. Despite a global decline in malaria mortality rates, there still remain challenges in many regions, particularly within sub-Saharan Africa, where the greatest level of mortality is evident<sup>1</sup>. Where effective drug treatments are available, the mortality that is associated with treatments for falciparum malaria is < 0.1 %<sup>2</sup>. However, where the parasite is able to multiply untamed, the parasite burden of the host increases resulting in organ dysfunction, impairment of higher brain function, loss of consciousness and anaemia, culminating in death.

A major shift in treatment strategies for malaria may be required, considering the increasing prevalence of anti-microbial resistance which has been exemplified by the emergence of resistance to chloroquine<sup>3</sup> and sulfadoxine/pyrimethamine (SP)<sup>4,5</sup>. Furthermore, the appearance of an artemisinin drug-resistance strain of malaria within the Greater Mekong Subregion (GMS), first identified in Cambodia in 2008<sup>6</sup>, poses particular concerns and demonstrates the need to explore alternative antimalarial agents. This is further highlighted by the increasing treatment failure associated with mefloquine and piperazine across the GMS<sup>7-10</sup>.

The 'Global Technical Strategy for Malaria'<sup>1</sup> comments on novel approaches required to aid malaria treatment and specifically focuses on opportunities for 'innovation in medicines', which provides a framework for the acceleration of malaria elimination. Given the complexity of current drug discovery and development strategies, consideration of existing, clinically approved, candidate molecules with a view to repurposing for malaria has many advantages. For example, the safety profile and clinical pharmacokinetics would have been established, and fast-track processes (e.g. FDA) allow for the establishment of new clinical indications<sup>11</sup>. Such approaches have found successes in the area of orphan diseases<sup>12</sup>, where specific unmet need exists and where traditional drug development strategies would be time-consuming. Ivermectin, is one potential candidate that may be suited for repurposing to malaria. Ivermectin is an endectocide and kills a range of parasites and associated vectors, and is currently marketed and licenced to treat onchocerciasis, lymphatic filariasis,

1  
2  
3  
4  
5  
6  
7  
8  
9  
10  
11  
12  
13  
14  
15  
16  
17  
18  
19  
20  
21  
22  
23  
24  
25  
26  
27  
28  
29  
30  
31  
32  
33  
34  
35  
36  
37  
38  
39  
40  
41  
42  
43  
44  
45  
46  
47  
48  
49  
50  
51  
52  
53  
54  
55  
56  
57  
58  
59  
60

78 strongyloidiasis, scabies and head lice <sup>13</sup>. The use of ivermectin in the treatment of  
79 onchocerciasis has been well documented over the past 25 years with community-wide mass  
80 drug administration (MDA) of ivermectin contributing to the near elimination of  
81 onchocerciasis <sup>14</sup>. Further, numerous studies have demonstrated that ivermectin can remain  
82 in the blood stream for a sufficiently long time-frame, following standard dosing, to kill the  
83 *Anopheline* vector <sup>15-19</sup> and malaria parasite <sup>20</sup>.

84 The importance of ivermectin as a potential novel drug for repurposing to malaria is  
85 exemplified by the formation of the ‘Ivermectin Research for Malaria Elimination Network’  
86 <sup>21</sup>, whose primary goal was to establish a common research agenda to aid in the generation of  
87 evidence base on which to support (or otherwise) whether ivermectin should be repurposed to  
88 malaria. Further we strongly recommend those wishing to gain an in-depth understanding of  
89 the repurposing ivermectin to consider a recent series of reviews exploring the  
90 pharmacokinetics evidence, regulatory policies and clinical development pathways to support  
91 the repurposing of ivermectin to malaria <sup>22-24</sup>

92 Ivermectin shows rapid absorption with an absorption half-life of 0.5-2.5 hours <sup>25,26</sup>, is highly  
93 lipophilic and is associated with extensive protein binding ( $f_u < 0.1$ ) and a large volume of  
94 distribution (3.1-3.5 L/kg) <sup>25</sup>. The metabolism of ivermectin is primarily mediated by  
95 Cytochrome P450 3A4 (CYP3A4) <sup>27</sup> and leads to a half-life of approximately 18 hours <sup>25</sup>. A  
96 complete description of the pharmacokinetics of ivermectin can be found in two review  
97 publications <sup>22,25</sup>. In clinical studies, ivermectin has been used across an extensive dosing  
98 range, with over 2.7 billion single doses of the 0.15-0.2 mg/kg dose administered through the  
99 Mectizan Donation program <sup>28</sup> as single doses. Furthermore, higher doses of up to 2 mg/kg  
100 as single doses have been administered <sup>29</sup> whilst the Centre for Disease Control and  
101 Prevention have recommended doses of up to 1.4 mg/kg for severe crusted scabies <sup>30</sup>. The  
102 wide safety profile would suggest higher doses are well tolerated. However, there are no  
103 current clinical trials assessing possible dosing regimens that could be used to identify an  
104 appropriate treatment regimen for use in malaria. A recent report has identified the  
105 ivermectin concentration capable of killing 50 % (LC50) mosquitoes as being approximately  
106 16 ng/mL <sup>31</sup>, which could be used as a first-principle potential target concentration for  
107 ‘therapeutic-effect’.

108 This manuscript, therefore, attempts to pragmatically assess the impact of possible dosing  
109 regimen designs on ivermectin plasma concentrations, with an emphasis on maintaining

plasma concentration above the LC50, through the application of physiologically-based pharmacokinetic (PBPK) modelling using virtual clinical trials.

The key objectives were therefore to: (i) assess the impact of dose escalation of ivermectin on adults (20-50 years old) and paediatrics within the age range of 3-5 years old, who pose significant challenges in treatment and are prone to developing severe malaria<sup>1</sup>; (ii) given that ivermectin is metabolised by CYP3A4, to assess the impact of induction based drug-drug interactions (DDIs) on reducing ivermectin plasma concentrations in adults and children and (iii) to illustrate the potential changes in ivermectin pharmacokinetics when dosed to a representative malaria population group originating from the GMS (i.e. Thailand).

## 2. METHODS

All population based PBPK modelling was conducted using the virtual clinical trials simulator Simcyp (Simcyp Ltd, a Certara company, Sheffield, UK, Version 16). Unless otherwise stated, mixed gender (50:50) populations were simulated. A six-stage workflow approach was applied for the development, validation and simulation of the ivermectin (Figure 1). The default Simcyp validated adult and paediatric 'healthy volunteer' population groups were used in simulations for Steps 1-5. The latter population group accounted for ontogenic related changes in physiological/biochemical parameters such as organ volumes, organ perfusion and drug metabolising enzymes<sup>32-34</sup>. Further, the Simcyp population groups account for population variability through the inclusion of a variability metric (% coefficient variability) which was established from public health data bases such as the US National health and Nutrition Examination Survey (<https://www.cdc.gov/nchs/nhanes/>).

### 2.1 Step 1: Base model development and validation

A full description of the model development can be found in Section 1 of the Supplementary Materials. For model development, clinical studies selected included: (i) single doses (30, 60, 90 and 120 mg) and multiple doses (30 mg and 60 mg daily for 7 days) in healthy subjects<sup>29</sup>; (ii) a single (tablet) 12 mg dose administered to healthy subjects<sup>35</sup>; (iii) a single 0.15 mg/kg dose administered to healthy subjects<sup>36</sup>; (iv) a single 0.20 mg/kg dose administered to healthy subjects<sup>37</sup>; a single 0.15 mg/kg dose administered to healthy subjects<sup>38</sup>; (v) single 0.15 mg/kg dose administered to onchocerciasis subjects<sup>39</sup>. A recent study by Ouédraogo et al. 2015<sup>40</sup> provided some additional ivermectin plasma concentration data, but this was excluded from the validation approaches due to the sparse nature of the data and the

141 lack of quantitative summary pharmacokinetics data (e.g  $C_{\max}$ ,  $t_{\max}$  and AUC) with which to  
142 directly compare.

143 Model development and refinement was conducted using the single and multiple doses  
144 studies in healthy subjects reported by Guzzo *et al.* (2002) <sup>29</sup> (clinical study (i) as detailed  
145 above). Model validation was subsequently assessed against clinical studies ii-v (as detailed  
146 above). In all cases, model simulations were run to match the reported age range and subject  
147 number as reported by each study.

148 Final ivermectin compound parameters that were applied to all subsequent steps are detailed  
149 in table 1, with the supplementary materials (Section 1) fully describing the approaches used  
150 to determine these parameter values.

## 151 **2.2 Step 2: Adult escalating dose study**

152 Previous ivermectin clinical studies have used single doses of between 1.4-2 mg/kg <sup>29 30</sup>, and  
153 therefore to define a potential upper limit of the therapeutic window, a single oral dose of 2  
154 mg/kg was administered using a Simcyp predefined healthy volunteer population with 100  
155 subjects. The upper therapeutic window band was estimated from the mean maximum  
156 concentration within the population group with the lower band set at the LC50 (16 ng/mL) <sup>31</sup>.

157 Subsequently, simulations were run using the healthy volunteer population aged 18-50 years  
158 (100 subjects) with ivermectin dosed orally at 0.15, 0.3 and 0.6 mg/kg as a single daily dose.  
159 Thereafter, the dose resulting in the greatest time above the LC50 (but below the upper limit  
160 of the therapeutic window) was selected and assessed under 3-day dosing and 5-day dosing,  
161 each with dosing intervals ( $\tau$ ) of 12- or 24-hours, representing dosing regimens that are  
162 widely used for common antimalarials such as artemether, lumefantrine and piperaquine <sup>31</sup>.  
163 Finally, the dosing regimen resulting in the greatest time above the LC50 was selected as the  
164 optimal dosing regimen in adults.

## 165 **2.3 Step 3: Paediatric escalating dose study**

166 Simulations were run using the Simcyp paediatric population group and designed to ensure  
167 simulations contained at least 100 subjects aged 3-5 years old and covering weight bandings  
168 of 15-25 kg. Dose escalation regimens were based on the optimal dose identified in adult  
169 population groups (Step 2) with the dosing regimen resulting in the greatest time above the  
170 LC50 selected as the optimal dosing regimen in paediatrics (healthy volunteer populations).



## 171 2.4 Step 4-5: Impact of induction-based drug-drug interactions on dosing strategies

172 Many malaria patients are often co-infected with other communicable diseases such as HIV  
173 <sup>41</sup>. In these cases, the pharmacotherapy requirements are often complex with multiple  
174 competing drug-drug interactions (DDIs) possible. Antiretroviral agents such as efavirenz  
175 have been demonstrated to induce the expression of CYP3A4 <sup>42-44</sup> and subsequently increase  
176 the metabolic clearance (and hence reduce plasma concentrations) of antimalarial agents <sup>45-48</sup>  
177 <sup>49</sup>. This may potentially increase the risk of malaria recrudescence and place the patients at  
178 risk of developing severe malaria. Therefore the potential risk of CYP3A4 induction on  
179 reducing the plasma concentration of ivermectin was assessed in this step.

180 Dosing strategies utilised weight-based dosing for adults (Step 4) and children (Step 5), with  
181 simulations run for between 15-21 days <sup>50,51</sup> with efavirenz dosed throughout the study  
182 duration (Adults: 600 mg once daily; Paediatrics: 250 mg once daily for 15 kg to < 20 kg and  
183 300 mg once daily for 20 kg to < 25 kg) and ivermectin dosing initiated at day 13, to ensure  
184 stable induction of CYP3A4 prior to ivermectin dosing. The impact of DDI was assessed  
185 through changes in the time above the LC50.

## 186 2.5 Step 6: Ivermectin dosing in a 'malaria-type' population group

187 To assess the impact of a potential changes in ivermectin pharmacokinetics when dosed in a  
188 non-Caucasian/Malaria infected population group, we utilised an Asian (Thailand) population  
189 group that was developed in a previous publication by our group to assess antimalarial  
190 pharmacokinetics within a malaria-infected population group <sup>51</sup>. This Thai population group  
191 was adapted to include appropriate geographical age-weight distributions for male and female  
192 adults and paediatrics. These adaptations also included revised blood biochemistry to match  
193 patient demographics identified within malaria patients. The development of this Thailand  
194 population group is fully described in the Supplementary Materials (Section 2). Simulations  
195 were performed based on optimal doses identified in previous sections.

## 196 2.6 Predictive performance

197 In all of the validation simulations (Step 1), predictions within 2-fold of the observed data  
198 were generally considered to represent an 'optimal' predictive performance and confirmed  
199 successful model development and validation, despite there being no uniform standard of  
200 acceptance to determine this criterion <sup>52-54</sup>. This 2-fold acceptance criterion was subsequently

1  
2  
3  
4  
5  
6  
7  
8  
9  
10  
11  
12  
13  
14  
15  
16  
17  
18  
19  
20  
21  
22  
23  
24  
25  
26  
27  
28  
29  
30  
31  
32  
33  
34  
35  
36  
37  
38  
39  
40  
41  
42  
43  
44  
45  
46  
47  
48  
49  
50  
51  
52  
53  
54  
55  
56  
57  
58  
59  
60

utilised in comparisons of simulated plasma-concentration profiles with published clinical data, where reported.

**2.7 Data and statistical analysis**

The observed data from clinical studies that were used for visual predictive checks were extracted using WebPlotDigitizer v.3.10 (<http://arohatgi.info/WebPlotDigitizer/>). Unless otherwise stated, all simulations employing weight-based dosing were run with 100-subject simulation in a 10x10 trial (10 subjects per trial with 10 trials) to account for reasonable inter-/intra individual variability being captured within the model simulations. Where necessary, pooling and post-processing of output Simcyp data were conducted to match individuals to the required age-weight boundary conditions for the study.

Where a DDI was simulated, the model performance was principally dictated by the comparison of the AUC ratio or C<sub>max</sub> ratio (ratio of the AUC or C<sub>max</sub> in the absence and presence of the efavirenz). An AUC ratio or C<sub>max</sub> ratio greater than 1.25 is indicative of an inhibition reaction whereas a ratio of less than 0.8 indicating an induction reaction whilst a ratio of between 0.8 – 1.25 indicating no interaction. Where applicable, statistical analysis was conducted using paired t-tests with a P < 0.05 indicating statistical significance.

**3. RESULTS**

**3.1 Step 1: Validation**

An ivermectin compound file was developed within Simcyp and validated against a range of published studies using the healthy volunteer population group. Model development considered a range of single<sup>29 35</sup> and multi-dose studies coupled with more traditional weight based dosing (0.15-0.20 mg/kg)<sup>36-39</sup>, and in all cases simulated ivermectin plasma concentration profiles were within the observed range for each study (Figure 2). Furthermore, the model predicted t<sub>max</sub>, C<sub>max</sub> and AUC were predicted to within 2-fold of the reported parameters for each study (Table 2) and confirmed successful model validation.

However, model predicted AUC<sub>0-t</sub> (AUC calculated from the study duration time only) was 3.9-fold underpredicted when compared to the study by Baraka *et al* (1996)<sup>36</sup> (Table 2). In contrast, model predicted AUC was within 2-fold when compared to that reported in the

study Okonkwo *et al* (1993)<sup>39</sup> for the same dose as that utilised by Baraka *et al* (1996)<sup>36</sup> (Table 2).

### 3.2 Step 2: Adult escalating dose study

Simulations were next performed to assess the impact of dosing-escalation on the time above the suggested LC50 (16 ng/ml). Single dose studies across a dosing range of 0.15-0.6 mg/kg (Figure 3A) resulted in a  $C_{\max}$  above the LC50 for all subjects, with higher doses resulting in a longer duration of time above the LC50, 10.4 hours for 0.15 mg/kg to 23 hours for 0.6 mg/kg (Table 3). A further dose of 2 mg/kg resulted in a  $C_{\max}$  of  $178.38 \pm 95.98$  ng/mL (Figure 3B) with a duration of time above the LC50 of greater than 24 hours (Table 3). Based upon the 2 mg/kg dose, the upper 'limit' of the therapeutic window was set at 435.30 ng/mL.

Under repeated daily dosing (once daily for 3 days), a similar trend of increasing time above the LC50 with an increasing dose (Table 3) was observed (Figure 3C). The 0.6 mg/kg dose resulted in time above the LC50 of 152.9 hours (Table 3). Extension of the dosing duration for the 0.6 mg/kg dose from a single daily dose for 3 days, to a twice daily for 3 days (Figure 3D) and twice daily dose for 5 days (Figure 3F) resulted in a significant increase in  $C_{\max}$  ( $P < 0.001$ ) and time above LC50 ( $151.51 \pm 66.22$  ng/mL and 178.24 hours to  $174.41 \pm 73.69$  ng/mL and 257.19 hours) compared to once daily dosing (Table 3).

### 3.3 Step 3: Paediatric escalating dose study

Simulations were next performed in healthy paediatric population groups aged 3-5 years to assess the impact of a dosing-escalation on the time above the suggested LC50 (16 ng/ml). As with adult populations, single dose studies across a dosing range of 0.15-0.6 mg/kg (Figure 4A) resulted in a  $C_{\max}$  above the LC50 which was dose dependant and resulted in a longer duration of time above the LC50, 10.1 hours for 0.15 mg/kg to 23.9 hours for 0.6 mg/kg (Table 4). With a higher dose of 2 mg/kg, a  $C_{\max}$  of  $348.40 \pm 148.95$  ng/mL was simulated (Figure 4B) which remained above the LC50 for greater than 24 hours (Table 4). Based upon a 2 mg/kg dose, the upper 'limit' of the therapeutic window was set at 516.91 ng/mL.

Repeated daily dosing (once daily for 3 days), resulted in a similar trend of increasing time above the LC50 (Figure 4C) (Table 4) with the largest dose (0.6 mg/kg) resulting in a time above the LC50 of 151.2 hours (Table 4).

1  
2  
3  
4  
5  
6  
7  
8  
9  
10  
11  
12  
13  
14  
15  
16  
17  
18  
19  
20  
21  
22  
23  
24  
25  
26  
27  
28  
29  
30  
31  
32  
33  
34  
35  
36  
37  
38  
39  
40  
41  
42  
43  
44  
45  
46  
47  
48  
49  
50  
51  
52  
53  
54  
55  
56  
57  
58  
59  
60

261 Upon extension of the dosing regimen from once daily for 3 days to either twice daily for 3  
262 days (Figure 4D), once daily for 5 days (Figure 4E) or twice daily for 5 days (Figure 4F), a  
263 significant increase in  $C_{max}$  ( $P < 0.001$ ) and time above LC50 compared to once daily dosing  
264 (Table 4) was simulated. The longest duration above the LC50 was determined for the twice  
265 daily 0.6 mg/kg dose for 5-days, 290.1 hours (Table 4).

266  
267  
268  
269  
270 **3.4 Step 4: Impact of induction-based drug-drug interactions on dosing strategies:**  
271 **adults**

272 To address the potential impact of malaria recrudescence in complex pharmacotherapy, e.g.  
273 HIV-coinfection, a DDI was simulated in the presence of the CYP3A4 inducer efavirenz,  
274 where the ivermectin dose was escalated. To ensure stable induction of CYP3A4, efavirenz  
275 was dosed throughout the simulation period with ivermectin dosing commencing on day 13  
276 onwards. Furthermore, dosing was conducted in such a fashion to ensure the ivermectin  $C_{max}$   
277 did not go beyond the upper therapeutic window identified in step 2.

278 For single daily doses, the impact of efavirenz on ivermectin pharmacokinetics generally  
279 resulted in an approximate 50 % decrease in ivermectin  $C_{max}$  (Figure 5A) ( $C_{max}$  ratio: 0.48)  
280 (Table 5) across all doses (0.15 mg/kg to 2 mg/kg) ( $P < 0.001$ ), with the highest dose  
281 resulting in a  $C_{max}$  of 120.39 ng/mL  $\pm$  61.70 ng/mL. Furthermore, the exposure of ivermectin  
282 in subjects was also significantly decreased (Figure 5A) with an approximate 75 % decrease  
283 in the AUC for across all doses (AUC ratio = 0.28) when compared to the absence of  
284 efavirenz ( $P < 0.0001$ ). The time above the LC50 compared to ivermectin alone (Table 3)  
285 was also significantly reduced for all equivalent doses ( $P < 0.001$ ), for example when  
286 comparing the 0.3 mg/kg dose daily for three days in the absence of efavirenz (time above  
287 LC50=86.2 h) (Table 3) to in the presence of efavirenz (time above LC50=19.7 h) (Table 5).

288 When dosing for 3-days (Figure 5B) or 5-days (Figure 5C),  $\tau$ =12 hours, the  $C_{max}$  was  
289 moderately higher than equivalent single daily doses, however an increase in the AUC was  
290 simulated which resulted in a significantly higher time above the LC50 for 3-days (1 mg/kg:  
291 77.3 hours; 2 mg/kg: 91.2 hours) or 5-day regimens (1 mg/kg: 138.8 hours; 2 mg/kg: 144.7

hours) compared to a single daily dose for three days (1 mg/kg: 30.8 hours; 2 mg/kg: 47.5 hours) (Table 5) ( $P<0.001$ ).

### 3.5 Step 5: Impact of induction-based DDIs on dosing strategies: paediatrics

The induction effects of efavirenz on CYP3A4 metabolism was further assessed in paediatric subjects, aged 3-5 years and spanning two efavirenz dosing bands (250 mg for 15 kg to < 20 kg) and 300 mg for 20 to < 25 kg).

For single daily doses, efavirenz exposure resulted in an approximate 57 % decrease in ivermectin  $C_{\max}$  (Figure 6A) ( $C_{\max}$  ratio: 0.43) (Table 6) across doses of 0.6, 1 and 2 mg/kg, with the highest dosing regimen (2 mg/kg for three days) resulting in a  $C_{\max}$  of 240.45 ng/mL  $\pm$  150.97 ng/mL. This was accompanied by an approximate 79 % decrease in the AUC across all doses (AUC ratio = 0.21) when compared to the absence of efavirenz. (Figure 6A) ( $P<0.001$ ). Furthermore, the time above the LC50 compared to ivermectin alone (Table 4) was also significantly reduced ( $P<0.001$ ), e.g. comparing the 0.60 mg/kg dose daily for three days in the absence of efavirenz (time above LC50=151.2 h) (Table 4) to in the presence of efavirenz (time above LC50=27.8 h) (Table 6).

When dosing twice daily for 3-days (Figure 6B) or 5-days (Figure 6C), the simulated  $C_{\max}$  was moderately higher (but not statistically significant) than the equivalent single daily doses (Table 6). This was however accompanied by an increase in the AUC which resulted in a significantly higher time above the LC50 for dosing of twice daily for 3-days (1 mg/kg: 81.2 hours; 2 mg/kg: 104.2 hours) or twice daily for 5-day regimens (1 mg/kg: 141.2 hours; 2 mg/kg: 142.2 hours) compared to a single daily dose for three days (1 mg/kg: 30.9 hours; 2 mg/kg: 30.9 hours) (Table 6).

### 3.6 Step 6: Ivermectin dosing in a 'malaria-type' population group

Although model simulations have been conducted in a healthy volunteer population group, which broadly follows demographic trends in the Caucasian population, the final stage of the modelling process considered the dosing of ivermectin within a non-Caucasian population group, using a custom designed Thailand malarial adult and paediatric population groups which was previously developed and applied to similar malaria modelling approaches by our group<sup>51</sup>, which had appropriate age-weight distributions and associated alterations to blood biochemistry. Ivermectin was dosed at 0.6 mg/kg once daily for three days to adult (Figure 7A) and paediatrics (Figure 7B). A noticeably lower ivermectin plasma concentrations were

1  
2  
3 323 simulated for the Thailand population group compared to the healthy volunteer group (Figure  
4 324 7A) with a similar  $C_{max}$  for each dose. However, the time above LC50 was significantly  
5  
6 325 reduced in the Thailand population compared to the healthy volunteer population ( $P<0.001$ )  
7  
8 326 (152 hours to 67.3 hours). This was however recoverable when the dosing regimen was  
9  
10 327 increased to 1 mg/kg and duration extended to once daily for 5 days, resulting in a  $C_{max}$  of  
11 328 176.12 ng/L  $\pm$  82.22 ng/mL and AUC of 4155.15 ng/mL.h  $\pm$  2230.82 ng/mL.h. Furthermore,  
12 329 the time above LC50 was 171.6 hours.

14  
15 330 The total oral clearance for ivermectin increased from 39.12 L/h  $\pm$  21.54 L/h for the  
16 331 Caucasian healthy adults to 45.2 L/h  $\pm$  27.41 L/h for the Thailand subjects.

18  
19 332 For paediatric subjects, the ivermectin plasma concentration profiles were general similar  
20 333 between Thailand and Caucasian healthy subjects, with a Thailand subjects showing a  
21 334 slightly lower time above LC50, 137.2 hours compared to Caucasian healthy subjects, 154.8  
22 335 hours (Figure 7B).

25  
26 336 **4. DISCUSSION**

27  
28 337 The eradication of malaria has been successful in many countries through the use of  
29 338 artemisinin-based combination therapy (ACT) <sup>1</sup>. However, this optimism has recently been  
30 339 tempered by the appearance of artemisinin-resistance *Plasmodium falciparum* strains in the  
31 340 GMS <sup>7-10</sup>. Despite the urgent need for new antimalarial agents to tackle this increasing risk of  
32 341 resistance, the time-lag associated with the discovery/development and clinical assessment of  
33 342 new drugs precludes the imminent regulatory approval of pipeline candidates <sup>55</sup>. However,  
34 343 drug repurposing provides an approach whereby existing licenced drugs can be ‘transferred’  
35 344 to an alternative (proven) indication, thereby bypassing the need for traditional  
36 345 discovery/development pipelines. Such approaches have indeed been useful in repurposing  
37 346 thalidomide to treat multiple myeloma <sup>56</sup> and crizotinib <sup>57</sup> for anaplastic lymphoma kinase  
38 347 gene-rearranged non-small cell lung cancer.

39  
40 348 Recent reports have highlighted ivermectin as a potential candidate for repurposing towards  
41 349 malaria <sup>22-24</sup>. Ivermectin is a dihydro derivate of avermectin and was initially licenced for use  
42 350 in veterinary medicines, but has demonstrated immense success in the treatment of  
43 351 Onchocerciasis in addition to a range of other nematode infections including Ascariasis,  
44 352 filariases, Gnathostomiasis and Trichuriasis <sup>58</sup>. Further, reports have also highlighted how  
45 353 ivermectin can remain in the blood stream for a sufficiently long time-frame to kill the  
46 354 *Anopheles* vector <sup>15-19</sup> and malaria parasite <sup>20</sup>. A key advantage of ivermectin therapy is that,



given its wide scale global use with many decades of monotherapy, there is yet to be confirmed scenarios of ivermectin resistance, leading to calls for ivermectin to be given consideration for other potential communicable diseases<sup>22-24,59</sup>.

The primary aim of this study was to explore the possible use of ivermectin dosing in adult and paediatric subjects using PBPK modelling through virtual clinical trials analysis. Such approaches have been previously employed by our group to explore the role of anti-malarial agents in special population groups such as paediatrics<sup>50</sup> and pregnant women<sup>51</sup>.

The primary objectives of this study were to: (i) assess the impact of dose escalation of ivermectin on adult (20-50 years old) and paediatric (3-5 years old) populations; (ii) assess the impact of inducted based drug-drug interactions on reducing ivermectin plasma concentrations in adults and children and (iii) to assess the impact of optimal dose of ivermectin on a representative malaria population group (Thailand).

The development of ivermectin as a compound file within Simcyp was focussed around utilising existing clinical studies reporting either full plasma concentration-time profiles or sparse sampling time-points with which to develop and drive appropriate predictions of ivermectin concentrations. The studies chosen represented a broad range of single<sup>29,35</sup> and multiple dose studies<sup>29</sup> coupled with standard<sup>36-39</sup> and higher dose studies<sup>29,35</sup>.

In the validation of the ivermectin compound file, it was necessary to address the role of active efflux on the intestinal drug absorption, particularly as ivermectin is known to be subjected to active efflux through P-glycoprotein<sup>60</sup>. However, in light of the lack of any *in-vitro* reported kinetic parameters describing active efflux, namely the apparent V<sub>max</sub> (maximum velocity) estimated for the carrier system (J<sub>max</sub>) and the Michaelis constant (K<sub>m</sub>), we incorporated an active efflux component for ivermectin through assuming the active efflux of ivermectin was initially similar to that of digoxin. The impact of this assumption was first confirmed through a sensitivity analysis (Supplementary materials: Section 1), which demonstrated that the choice of digoxin *in vitro* transporter-mediated intrinsic clearance (CL<sub>intP-glycoprotein</sub>) of 2.5 µL/min, and associated relative activity factor (0.1) was sufficient to capture an appropriate t<sub>max</sub> and C<sub>max</sub> for a 60 mg single dose of ivermectin<sup>61</sup>.

This approach was further extended to all model simulations in Step 1, and demonstrated successful validation for clinical studies ii-v (see section 2.1) (Figure 2), with all predicted pharmacokinetic parameters residing within the range of literature reported values for all

dosing regimens simulated, and in particular the  $C_{\max}$ ,  $t_{\max}$  and AUC predictions all within 2-fold of those reported by each clinical study (Table 2).

However, model simulations were unable to capture the  $AUC_{0-t}$  reported by Baraka *et al* (1996)<sup>36</sup>. It is possible that the mismatch may have been attributed to the population group utilised for the Baraka study, namely Sudanese, where age-weight relationships have highlighted an overall lower adult weight compared to healthy volunteers (Caucasian) populations<sup>62</sup>. It is also unclear from the Baraka study whether  $AUC_{0-t}$  or  $AUC_{\text{inf}}$  (AUC extrapolated to infinity) was reported. Furthermore, despite this underprediction, our model predicted  $AUC_{0-t}$  was within 2-fold of that reported by Okonkwo *et al* (1993)<sup>39</sup>, which utilised an identical dose and dosing regimen as Baraka *et al* (1996)<sup>36</sup>.

Having successfully demonstrated validation of the ivermectin compound file, we next assessed the impact of dose-escalation on the both the  $C_{\max}$ , exposure (AUC) and time above the LC50 (16 ng/mL)<sup>31</sup>. Although a key metric for success with antimalarial agents is the day-7 concentration, this information is lacking with ivermectin. The LC50 provides a suitable metric with which to develop an 'exposure-time' relationship. Whilst this has not been fully described within malaria subjects, recent reports have identified LC50 for *Anopheles minimus* (LC50 = 16.3 ng/ml), *Anopheles campestris* (LC50 = 26.4 ng/ml), *Anopheles sawadwongporni* (LC50 = 26.9 ng/ml) and *Anopheles. dirus* (LC50 = 55.6 ng/ml)<sup>31</sup>. Given that *Anopheles minimus* is the primary malaria vector within the GMS<sup>63</sup>, it was assumed that an LC50 of 16 ng/mL would form the lower spectrum of a potential therapeutic window. Weight-based dose-escalation over 0.15 mg/kg (standard dose) to 0.60 mg/kg for single doses (Figure 3A) resulted in a clear increase in  $C_{\max}$  and time above the LC50 (Table 3), with a higher dose of 2 mg/kg (Figure 3B) resulting in a time above the LC50 > 24 hours (Table 3).

A 2 mg/kg dose have been previously clinically administered<sup>29</sup>, with the Centre for Disease Control and Prevention recommending doses of up to 1.4 mg/kg for severe crusted scabies<sup>30</sup>. Here, we assumed that a dose of 2 mg/kg would be a realistic 'safe' maximum upper daily dose, given that it was clinically used with no serious adverse reactions in subjects<sup>29</sup>. It was decided to set the upper limit of a possible therapeutic window at the population simulated mean  $C_{\max}$ , 435.20 ng/mL for adults and 516.91 ng/mL for children.

Therefore, assuming the therapeutic window ranged from 16 ng/mL to 435.20 ng/mL (or 516.91 ng/mL for paediatrics), we assessed the impact of multiple dosing regimens on time



above the LC50 (Figure 3C-F). As expected, a decrease in dosing interval ( $\tau$ = 24 hours to 12 hours) and increase in dosing regimen duration (3-days or 5 days) resulted in a proportional increase in  $C_{\max}$  and time above LC50 (Table 3). However, the overall increase in the  $C_{\max}$  was minimal when comparing single doses with equivalent doses over 3 days (e.g. 0.6 mg/kg single dose: 95.86 ng/mL  $\pm$  31.72 ng/mL and daily for 3 days 113.11 ng/mL  $\pm$  39.54 ng/mL (Table 3). This was accompanied by an increase in the overall exposure (e.g. 0.6 mg/kg single dose: 960.29 ng/mL.h  $\pm$  335.66 ng/mL.h and daily for 3 days 3581.99 ng/mL.h  $\pm$  1777.58 ng/mL.h) and associated with an increase in the LC50 from 23.2 hours to 152.9 hours. Thus, the extension of a treatment duration from a single dose to a three-day or five-day treatment regimen would significantly enhance overall ivermectin exposure within the therapeutic window and enhance exposure for approximately 7-11 days. Multiple dosing regimens have previously been used on *Onchocerca volvulus*<sup>64,65</sup> and *Wuchereria bancrofti*<sup>66</sup> and which has been well tolerated.

A key benefit of PBPK modelling is the ability to pragmatically assess the pharmacokinetics of a drug in different population groups, and we next predicted the potential pharmacokinetics in children aged 3-5 years, primarily based upon the recommended weight minimum weight of 15 kg. We attempted to develop both an appropriate therapeutic range in paediatrics and identify the optimal treatment regimens to prolong the time above the LC50. We utilised the same dosing approaches as adults and identified 516.91 ng/mL, as being the potential upper limit for a proposed therapeutic window, based upon doing at 2 mg/kg. Although this is dosing regimen used in adults, it is below the dose of approximately 7-8 mg/kg used in reports of a child who demonstrated ivermectin toxicity<sup>67</sup>.

As with adults, increasing single doses (Figure 4A) resulted in increases in  $C_{\max}$  and AUC with a longer time above the LC50 (Table 4). Furthermore, a similar increase in dosing interval and duration (Figure 4C-E) resulting in a proportional increase in time above the LC50 (Table 4), with the 0.6 mg/kg twice daily for 5 days resulting in the longest time above the LC50 (290.1 ng/mL or 41.4 days), similar to that obtained in adults, 257.19 hours (Table 3).

Thus, for both adults and children, a higher dose of 0.6 mg/kg administered twice daily for 3 or 5 days, leads to significantly higher  $C_{\max}$  values compared to their corresponding single

1  
2  
3  
4  
5  
6  
7  
8  
9  
10  
11  
12  
13  
14  
15  
16  
17  
18  
19  
20  
21  
22  
23  
24  
25  
26  
27  
28  
29  
30  
31  
32  
33  
34  
35  
36  
37  
38  
39  
40  
41  
42  
43  
44  
45  
46  
47  
48  
49  
50  
51  
52  
53  
54  
55  
56  
57  
58  
59  
60

451 daily doses whilst also providing a longer duration above the LC50. When considering the  
452 potential problem of the lack of medication compliance with extended dosing of medicines, a  
453 3-day regimen may be an appropriate dosing regimen administered twice daily, to ensure  
454 prolonged duration above the LC50 of 9-11 days.

455 Under standard dosing conditions, a 3-day regimen may be an appropriate way to ensuring  
456 prolonged effects. However, many malaria patients are often co-infected with other  
457 communicable diseases such as Tuberculosis <sup>41,68-70</sup> or HIV <sup>41</sup>. In these cases, the  
458 pharmacotherapy requirements are often complex with multiple competing drug-drug  
459 interactions (DDIs) possible. Previously we have illustrated the impact of induction-based  
460 DDIs on the reducing the plasma concentration of lumefantrine under dosing with rifampicin  
461 (a CYP3A4 inducer) <sup>50</sup>, and this step next considered a similar DDI with the use of the  
462 antiretroviral efavirenz to simulate HIV-coinfected malaria subjects to ultimately assess the  
463 impact of the DDI on reducing ivermectin plasma concentrations.

464 In all simulations with adults (Figure 5) or paediatrics (Figure 6), the exposure to efavirenz  
465 (250 mg once daily for 15 kg to < 20 kg and 300 mg once daily for 20 kg to < 25 kg)  
466 significantly reduced ivermectin C<sub>max</sub>, exposure (AUC) and time above the LC50 for all  
467 dosing regimens (Table 5 and 6). The impact of this DDI can be assessed through the AUC  
468 ratio or C<sub>max</sub> ratio, which indicate significant decreases in both AUC ratio (0.21-0.28) and  
469 C<sub>max</sub> ratio (0.39-0.48) for adult studies (Table 5) and a greatest decrease in paediatrics (AUC:  
470 0.19-0.21; C<sub>max</sub>: 0.36-0.43) (Table 6) across all dosing regimens.

471 In trying to overcome the reduced exposure of ivermectin in the presence of a CYP3A4  
472 inducer, the use of 1 mg/kg or 2 mg/kg twice daily for five days in adults and children would  
473 achieve the greatest time above the LC50 (adults: 138.8 hours and 144.7 hours respectively;  
474 paediatrics: 141.2 hours and 142.1 hours respectively).

475 The focus of this study has generally been towards establishing appropriate dosing regimens  
476 for ivermectin for use in malaria infected subjects. However, the marked differences in  
477 global age-body weight relationships <sup>62</sup> would clearly alter the establishment of dosing  
478 regimens and would, in theory, render a ‘one-dose-fits-all’ approach inappropriate. Our  
479 group has recently utilised a geographic-region specific malaria population group for virtual  
480 clinical trials simulation <sup>51</sup>. We adapted this population group for use in the present study  
481 and developed a simplistic representative Thailand population group with appropriate body  
482 weight distribution for adults and paediatric subjects, whilst also incorporating appropriate

changes in blood biochemistry often observed in malaria-infected patients<sup>51</sup>. Using this approach, we demonstrated a significant difference in the simulated ivermectin plasma concentration from a 0.60 mg/kg daily dose for 3 days regimen (Figure 7A), with a statistically significant 84.7 hours decrease in the time above LC50 in the Thailand population compared to the healthy volunteer population. As dosing was focused on weight-based approaches, the differences in the median body weight for the simulated Thailand population group, 49.86 kg  $\pm$  10.25 kg, compared to the healthy volunteer group, 69.41 kg  $\pm$  14.29 kg, would therefore alter resultant ivermectin plasma concentration and exemplified the needs to consider population-based age-weight distribution data, as exemplified by the study by Hayes *et al* (2015)<sup>62</sup>, to develop more appropriate weight-based dosing regimen for malaria endemic regions. By addressing this potential disparity between body weights, the dosing regimen was adapted to 1 mg/kg, and this could recapture the time above LC50 to a similar extent as that observed in the healthy volunteer population group (Figure 7A). It should be noted that the neutral charge of ivermectin would likely result in preferential binding to human serum albumin (HSA). However, HSA is known to decrease in malaria subjects along with changes in both the haematocrit and alpha-one acidic glycoprotein<sup>51</sup>. This decrease in HSA would be expected to increase both the volume of distribution of ivermectin and more importantly, alter its hepatic extraction, particularly given that ivermectin is highly protein bound<sup>71</sup>. An analysis of the oral clearance demonstrated a significant ( $P < 0.01$ ) increase in Thailand subjects compared to healthy volunteers, and this also accounts for the lower overall plasma concentrations. Interesting, a similar trend was not observed in the paediatric population, with simulated ivermectin concentration broadly similar in both population group (Figure 7B)

It should, however, be noted that currently marketed ivermectin contains a mixture termed ivermectin B1a, consisting of an ethyl group at the C-26 position, and ivermectin B1b containing a methyl group<sup>72</sup>, in an at least 80% B1a and no more than 20 % B1b mixture<sup>73</sup>. Thus, the possibility of wide variability in ivermectin form within each dosing unit may introduce a wide variation of clinical dose response. Given the possibility of a relatively wide therapeutic window, the impact of such variability may be contained. However further work is required to define the exact duration above the LC50 required to sustain an effect.

The work presented in this study demonstrates the application of PBPK modelling to the successful development and validation of a PBPK model for ivermectin. This has allowed the pragmatic assessment of different dosing regimen designs on ivermectin plasma concentrations *in liue* of clinical trials. Whilst the work presented in this study is not intended to replace future clinical trials assessment of ivermectin in the context of malaria treatment, it can be used to guide and assess other novel dosing regimens or in complex special population groups. However, despite the large number of clinical studies in adults, there is a distinct sparsity in the availability of clinical studies examining ivermectin pharmacokinetics in children, and to fully exploit ivermectin in the context of malaria, urgent clinical trials are required to assess the safety and efficacy of ivermectin in children at doses identified within this study for use in malaria, particularly in the event of an CYP3A4-mediated induction DDI.

Further, the lack of kinetic parameters for P-glycoprotein efflux ( $J_{\max}$  and  $k_m$ ) would warrant attention placed on elucidating appropriate *in-vitro* Caco-2 P-glycoprotein kinetic efflux parameters to improve future model predictions. However, using the kinetic parameters associated with digoxin efflux, the model was able appropriately capture this efflux *ab orally* and yield estimates suitable estimates of  $t_{\max}$  during the model development and for all clinical studies used during the validation stage (Step 1). The model provided will therefore allow for future refinement when this information becomes available.

Given that ivermectin is a highly lipophilic compound<sup>74</sup>, it is likely that its oral absorption and oral bioavailability will be enhanced with fat-rich meals, in a similar fashion to other antimalarial agents, e.g. artemether<sup>75,76</sup> and lumefantrine<sup>76</sup>. This would also require consideration of the impact of biorelevant 'fed' dissolution media on the *in-vitro* dissolution rate of ivermectin from a solid dosage formulation. Such data is lacking for the majority of currently used antimalarial agents, and if determined for ivermectin, the proposed model can be adapted to include cumulative percentage release information for fasted and fed states which will allow exploration of the impact of fat-rich meals on ivermectin solubility and dissolution.

## CONCLUSION

Although malaria eradication has had wide ranging global successes, the appearance of artemisinin-based combination therapy resistance in the GMS requires urgent attention to the development of new anti-malarial drugs. Traditional discovery/development pipelines may

not accommodate the swift reaction that is required, and repurposing of alternative drug therapies may provide a novel approach to discover new therapies for malaria. Ivermectin is one such drug which has gained attention as a potential candidate. This study has further added to the understanding of the possibility of using ivermectin in a clinical setting within diverse population groups. The dosing regimens simulated are similar to existing therapeutic regimens, and given the wide therapeutic dosing range, provides further support for the repurposing of ivermectin to malaria.

## ACKNOWLEDGEMENTS

This research did not receive any specific grant from funding agencies in the public, commercial, or not-for-profit sectors.

## REFERENCES

1. Organization WH 2016. Global Technical Strategy for Malaria 2016–2030. 2015. Geneva 35pp.
2. White NJ 2004. Antimalarial drug resistance. *Journal of Clinical Investigation* 113(8):1084-1092.
3. Payne D 1987. Spread of chloroquine resistance in *Plasmodium falciparum*. *Parasitology today (Personal ed)* 3(8):241-246.
4. Roper C, Pearce R, Bredenkamp B, Gumedde J, Drakeley C, Mosha F, Chandramohan D, Sharp B 2003. Antifolate antimalarial resistance in southeast Africa: a population-based analysis. *Lancet (London, England)* 361(9364):1174-1181.
5. Nair S, Williams JT, Brockman A, Paiphun L, Mayxay M, Newton PN, Guthmann JP, Smithuis FM, Hien TT, White NJ, Nosten F, Anderson TJ 2003. A selective sweep driven by pyrimethamine treatment in southeast asian malaria parasites. *Molecular biology and evolution* 20(9):1526-1536.
6. Dondorp AM, Nosten F, Yi P, Das D, Phyo AP, Tarning J, Lwin KM, Arie F, Hanpithakpong W, Lee SJ, Ringwald P, Silamut K, Imwong M, Chotivanich K, Lim P, Herdman T, An SS, Yeung S, Singhasivanon P, Day NPJ, Lindegardh N, Socheat D, White NJ 2009. Artemisinin Resistance in *Plasmodium falciparum* Malaria. *New England Journal of Medicine* 361(5):455-467.
7. Spring MD, Lin JT, Manning JE, Vanachayangkul P, Somethy S, Bun R, Se Y, Chann S, Ittiverakul M, Sia-ngam P, Kuntawunginn W, Arsanok M, Buathong N, Chaorattanakawee S, Gosi P, Ta-aksorn W, Chanarat N, Sundrakes S, Kong N, Heng TK, Nou S, Teja-isavadharm P, Pichyangkul S, Phann ST, Balasubramanian S, Juliano JJ, Meshnick SR, Chour CM, Prom S, Lanteri CA, Lon C, Saunders DL 2015. Dihydroartemisinin-piperaquine failure associated with a triple mutant including kelch13 C580Y in Cambodia: an observational cohort study. *The Lancet Infectious Diseases* 15(6):683-691.
8. Leang R, Taylor WR, Bouth DM, Song L, Tarning J 2015. Evidence of *Plasmodium falciparum* Malaria Multidrug Resistance to Artemisinin and Piperaquine in Western



- 587 Cambodia: Dihydroartemisinin-Piperaquine Open-Label Multicenter Clinical Assessment.
- 588 59(8):4719-4726.
- 589 9. Phyto AP, Ashley EA, Anderson TJC, Bozdech Z, Carrara VI, Sripawat K, Nair S,
- 590 White MM, Dziekan J, Ling C, Proux S, Konghahong K, Jeeyapant A, Woodrow CJ,
- 591 Imwong M, McGready R, Lwin KM, Day NPJ, White NJ, Nosten F 2016. Declining Efficacy
- 592 of Artemisinin Combination Therapy Against *P. falciparum* Malaria on the Thai–Myanmar
- 593 Border (2003–2013): The Role of Parasite Genetic Factors. *Clinical Infectious Diseases*
- 594 63(6):784-791.
- 595 10. Amaratunga C, Lim P, Suon S, Sreng S, Mao S, Sopha C, Sam B, Dek D, Try V,
- 596 Amato R, Blessborn D, Song L, Tullo GS, Fay MP, Anderson JM, Tarning J, Fairhurst RM
- 597 2016. Dihydroartemisinin–piperaquine resistance in *Plasmodium falciparum* malaria in
- 598 Cambodia: a multisite prospective cohort study. *The Lancet Infectious Diseases* 16(3):357-
- 599 365.
- 600 11. Lotharius J, Gamo-Benito FJ, Angulo-Barturen I, Clark J, Connelly M, Ferrer-Bazaga
- 601 S, Parkinson T, Viswanath P, Bhandodkar B, Rautela N, Bharath S, Duffy S, Avery VM,
- 602 Möhrle JJ, Guy RK, Wells T 2014. Repositioning: the fast track to new anti-malarial
- 603 medicines? *Malaria journal* 13(1):143.
- 604 12. Sardana D, Zhu C, Zhang M, Gudivada RC, Yang L, Jegga AG 2011. Drug
- 605 repositioning for orphan diseases. *Briefings in Bioinformatics* 12(4):346-356.
- 606 13. Ōmura S, Crump A 2017. Ivermectin and malaria control. *Malaria journal* 16(1):172.
- 607 14. Richards FO 2017. Upon entering an age of global ivermectin-based integrated mass
- 608 drug administration for neglected tropical diseases and malaria. *Malaria journal* 16(1):168.
- 609 15. Tesh RB, Guzman H 1990. Mortality and infertility in adult mosquitoes after the
- 610 ingestion of blood containing ivermectin. *The American journal of tropical medicine and*
- 611 *hygiene* 43(3):229-233.
- 612 16. Chaccour C, Lines J, Whitty CJ 2010. Effect of ivermectin on *Anopheles gambiae*
- 613 mosquitoes fed on humans: the potential of oral insecticides in malaria control. *The Journal*
- 614 *of infectious diseases* 202(1):113-116.
- 615 17. Kobylinski KC, Deus KM, Butters MP, Hongyu T, Gray M, da Silva IM, Sylla M,
- 616 Foy BD 2010. The effect of oral anthelmintics on the survivorship and re-feeding frequency
- 617 of anthropophilic mosquito disease vectors. *Acta tropica* 116(2):119-126.
- 618 18. Kobylinski KC, Sylla M, Chapman PL, Sarr MD, Foy BD 2011. Ivermectin mass
- 619 drug administration to humans disrupts malaria parasite transmission in Senegalese villages.
- 620 *The American journal of tropical medicine and hygiene* 85(1):3-5.
- 621 19. Foy BD, Kobylinski KC, da Silva IM, Rasgon JL, Sylla M 2011. Endectocides for
- 622 malaria control. *Trends in parasitology* 27(10):423-428.
- 623 20. Panchal M, Rawat K, Kumar G, Kibria K, Singh S, Kalamuddin M, Mohammed A,
- 624 Malhotra P, Tuteja R 2014. *Plasmodium falciparum* signal recognition particle components
- 625 and anti-parasitic effect of ivermectin in blocking nucleo-cytoplasmic shuttling of SRP. *Cell*
- 626 *death & disease* 5(1):e994.
- 627 21. Chaccour CJ, Rabinovich NR, Slater H, Canavati SE, Bousema T, Lacerda M, ter
- 628 Kuile F, Drakeley C, Bassat Q, Foy BD, Kobylinski K 2015. Establishment of the Ivermectin
- 629 Research for Malaria Elimination Network: updating the research agenda. *Malaria journal*
- 630 14(1):243.
- 631 22. Chaccour C, Hammann F, Rabinovich NR 2017. Ivermectin to reduce malaria
- 632 transmission I. Pharmacokinetic and pharmacodynamic considerations regarding efficacy and
- 633 safety. *Malaria journal* 16(1):161.
- 634 23. Chaccour C, Rabinovich NR 2017. Ivermectin to reduce malaria transmission II.
- 635 Considerations regarding clinical development pathway. *Malaria journal* 16(1):166.

24. Chaccour C, Rabinovich NR 2017. Ivermectin to reduce malaria transmission III. Considerations regarding regulatory and policy pathways. *Malaria journal* 16(1):162.
25. Canga AG, Prieto AMS, Liébana MJD, Martínez NF, Vega MS, Vieitez JGG 2008. The pharmacokinetics and interactions of ivermectin in humans—a mini-review. *The AAPS journal* 10(1):42-46.
26. Edwards G, Dingsdale A, Helsby N, Orme ME, Breckenridge A 1988. The relative systemic availability of ivermectin after administration as capsule, tablet, and oral solution. *European journal of clinical pharmacology* 35(6):681-684.
27. Zeng Z, Andrew N, Arison B, Luffer-Atlas D, Wang R 1998. Identification of cytochrome P4503A4 as the major enzyme responsible for the metabolism of ivermectin by human liver microsomes. *Xenobiotica; the fate of foreign compounds in biological systems* 28(3):313-321.
28. Lawrence J, Sodahlon YK, Ogooussan KT, Hopkins AD 2015. Growth, Challenges, and Solutions over 25 Years of Mectizan and the Impact on Onchocerciasis Control. *PLOS Neglected Tropical Diseases* 9(5):e0003507.
29. Guzzo CA, Furtek CI, Porras AG, Chen C, Tipping R, Clineschmidt CM, Sciberras DG, Hsieh JYK, Lasseeter KC 2002. Safety, tolerability, and pharmacokinetics of escalating high doses of ivermectin in healthy adult subjects. *The Journal of Clinical Pharmacology* 42(10):1122-1133.
30. CDC. 2016. Prescription medication for the treatment of scabies. . ed., USA.
31. Kobylinski KC, Ubalee R, Ponlawat A, Nitatsukprasert C, Phasomkulsolsil S, Wattanakul T, Tarning J, Na-Bangchang K, McCardle PW, Davidson SA, Richardson JH 2017. Ivermectin susceptibility and sporontocidal effect in Greater Mekong Subregion Anopheles. *Malaria journal* 16(1):280.
32. Johnson TN 2005. Modelling approaches to dose estimation in children. *Brit J Clin Pharmacol* 59(6):663-669.
33. Johnson TN 2008. The problems in scaling adult drug doses to children. *Archives of disease in childhood* 93(3):207-211.
34. Small BG, Wendt B, Jamei M, Johnson TN 2017. Prediction of liver volume - a population-based approach to meta-analysis of paediatric, adult and geriatric populations - an update. *Biopharmaceutics & drug disposition*.
35. Edwards G, Dingsdale A, Helsby N, Orme ML, Breckenridge AM 1988. The relative systemic availability of ivermectin after administration as capsule, tablet, and oral solution. *European journal of clinical pharmacology* 35(6):681-684.
36. Baraka OZ, Mahmoud BM, Marschke CK, Geary TG, Homeida MMA, Williams JF 1996. Ivermectin distribution in the plasma and tissues of patients infected with *Onchocerca volvulus*. *European journal of clinical pharmacology* 50(5):407-410.
37. Na-Bangchang K, Banmairuroi V, Choemung A 2006. High-performance liquid chromatographic method for the determination of ivermectin in plasma. *Southeast Asian J Trop Med Public Health* 37(5):848-858.
38. Njoo FL, Beek WMJ, Keukens HJ, Van Wilgenburg H, Oosting J, Stilma JS, Kijlstra A 1995. Ivermectin Detection in Serum of Onchocerciasis Patients: Relationship to Adverse Reactions. *The American Journal of Tropical Medicine and Hygiene* 52(1):94-97.
39. Okonkwo PO, Ogbuokiri JE, Ofoegbu E, Klotz U 1993. Protein binding and ivermectin estimations in patients with onchocerciasis. *Clinical Pharmacology & Therapeutics* 53(4):426-430.
40. Ouédraogo AL, Bastiaens GJH, Tiono AB, Guelbéogo WM, Kobylinski KC, Ouédraogo A, Barry A, Bougouma EC, Nebie I, Ouattara MS, Lanke KHW, Fleckenstein L, Sauerwein RW, Slater HC, Churcher TS, Sirima SB, Drakeley C, Bousema T 2015. Efficacy and Safety of the Mosquitocidal Drug Ivermectin to Prevent Malaria Transmission After

- 686 Treatment: A Double-Blind, Randomized, Clinical Trial. *Clinical Infectious Diseases*  
687 60(3):357-365.
- 688 41. Jegede FE, Oyeyi TI, Abdulrahman SA, Mbah HA, Badru T, Agbakwuru C,  
689 Adedokun O 2017. Effect of HIV and malaria parasites co-infection on immune-  
690 hematological profiles among patients attending anti-retroviral treatment (ART) clinic in  
691 Infectious Disease Hospital Kano, Nigeria. *PLoS One* 12(3):e0174233.
- 692 42. Habtewold A, Amogne W, Makonnen E, Yimer G, Nylén H, Riedel KD 2013.  
693 Pharmacogenetic and pharmacokinetic aspects of CYP3A induction by efavirenz in HIV  
694 patients. *Pharmacogenomics J* 13.
- 695 43. Hariparsad N, Nallani SC, Sane RS, Buckley DJ, Buckley AR, Desai PB 2004.  
696 Induction of CYP3A4 by efavirenz in primary human hepatocytes: comparison with rifampin  
697 and phenobarbital. *Journal of clinical pharmacology* 44(11):1273-1281.
- 698 44. Mouly S, Lown KS, Kornhauser D, Joseph JL, Fiske WD, Benedek IH, Watkins PB  
699 2002. Hepatic but not intestinal CYP3A4 displays dose-dependent induction by efavirenz in  
700 humans. *Clinical Pharmacology & Therapeutics* 72(1):1-9.
- 701 45. Byakika-Kibwika P, Lamorde M, Mayito J, Nabukeera L, Namakula R, Mayanja-  
702 Kizza H 2012. Significant pharmacokinetics interactions between artemether/lumefantrine  
703 and efavirenz or in HIV-infected Ugandan adults. *J Antimicrob Chemother* 67.
- 704 46. Fillekes Q, Natukunda E, Balungi J, Kendall L, Bwakura-Dangarembizi M,  
705 Keishanyu R, Ferrier A, Lutakome J, Gibb DM, Burger DM, Walker AS 2011. Pediatric  
706 underdosing of efavirenz: a pharmacokinetic study in Uganda. *J Acquir Immune Defic Syndr*  
707 58(4):392-398.
- 708 47. Huang L, Parikh S, Rosenthal PJ, Lizak P, Marzan F, Dorsey G 2012. Concomitant  
709 efavirenz reduces pharmacokinetic exposure to the antimalarial drug artemether-lumefantrine  
710 in healthy volunteers. *J Acquir Immune Defic Syndr* 61.
- 711 48. Maganda BA, Minzi OM, Ngaimisi E, Kamuhabwa AA, Aklillu E 2016. CYP2B6\*6  
712 genotype and high efavirenz plasma concentration but not nevirapine are associated with low  
713 lumefantrine plasma exposure and poor treatment response in HIV-malaria-coinfected  
714 patients. *Pharmacogenomics J* 16(1):88-95.
- 715 49. Maganda BA, Ngaimisi E, Kamuhabwa AA, Aklillu E, Minzi OM 2015. The  
716 influence of nevirapine and efavirenz-based anti-retroviral therapy on the pharmacokinetics  
717 of lumefantrine and anti-malarial dose recommendation in HIV-malaria co-treatment. *Malaria*  
718 *journal* 14(1):179.
- 719 50. Olafuyi O, Coleman M, Badhan RKS 2017. Development of a paediatric  
720 physiologically based pharmacokinetic model to assess the impact of drug-drug interactions  
721 in tuberculosis co-infected malaria subjects: A case study with artemether-lumefantrine and  
722 the CYP3A4-inducer rifampicin. *Eur J Pharm Sci* 106:20-33.
- 723 51. Olafuyi O, Coleman M, Badhan RKS 2017. The application of physiologically based  
724 pharmacokinetic modelling to assess the impact of antiretroviral-mediated drug-drug  
725 interactions on piperazine antimalarial therapy during pregnancy.
- 726 52. Ginsberg G, Hattis D, Russ A, Sonawane B 2004. Physiologically based  
727 pharmacokinetic (PBPK) modeling of caffeine and theophylline in neonates and adults:  
728 Implications for assessing children's risks from environmental agents. *Journal of Toxicology*  
729 *and Environmental Health-Part a-Current Issues* 67(4):297-329.
- 730 53. Edginton AN, Schmitt W, Willmann S 2006. Development and evaluation of a  
731 generic physiologically based pharmacokinetic model for children. *Clinical Pharmacokinetics*  
732 45(10):1013-1034.
- 733 54. Parrott N, Davies B, Hoffmann G, Koerner A, Lave T, Prinssen E, Theogaraj E,  
734 Singer T 2011. Development of a Physiologically Based Model for Oseltamivir and



- Simulation of Pharmacokinetics in Neonates and Infants. *Clinical Pharmacokinetics* 50(9):613-623.
55. White NJ 2010. Artemisinin resistance—the clock is ticking. *The Lancet* 376(9758):2051-2052.
56. Breitkreutz I, Anderson KC 2008. Thalidomide in multiple myeloma--clinical trials and aspects of drug metabolism and toxicity. *Expert opinion on drug metabolism & toxicology* 4(7):973-985.
57. Shaw AT, Yasothan U, Kirkpatrick P 2011. Crizotinib. *Nat Rev Drug Discov* 10(12):897-898.
58. Ottesen EA, Campbell WC 1994. Ivermectin in human medicine. *The Journal of antimicrobial chemotherapy* 34(2):195-203.
59. Speare R, Durrheim D 2004. Mass treatment with ivermectin: an underutilized public health strategy. *Bulletin of the World Health Organization* 82(8):562.
60. Kigen G, Edwards G 2017. Drug-transporter mediated interactions between anthelmintic and antiretroviral drugs across the Caco-2 cell monolayers. *BMC Pharmacology and Toxicology* 18(1):20.
61. Guzzo CA, Furtek CI, Porras AG, Chen C, Tipping R, Clineschmidt CM, Sciberras DG, Hsieh JY, Lasseter KC 2002. Safety, tolerability, and pharmacokinetics of escalating high doses of ivermectin in healthy adult subjects. *Journal of clinical pharmacology* 42(10):1122-1133.
62. Hayes DJ, van Buuren S, ter Kuile FO, Stasinopoulos DM, Rigby RA, Terlouw DJ 2015. Developing regional weight-for-age growth references for malaria-endemic countries to optimize age-based dosing of antimalarials. *Bulletin of the World Health Organization* 93(2):74-83.
63. Yu G, Yan G, Zhang N, Zhong D, Wang Y, He Z, Yan Z, Fu W, Yang F, Chen B 2013. The Anopheles community and the role of Anopheles minimus on malaria transmission on the China-Myanmar border. *Parasites & Vectors* 6(1):264.
64. Duke BOL, Zea-Flores G, Castro J, Cupp EW, Muñoz B 1990. Effects of Multiple Monthly Doses of Ivermectin on Adult Onchocerca volvulus. *The American Journal of Tropical Medicine and Hygiene* 43(6):657-664.
65. Chavasse DC, Post RJ, Lemoh PA, Whitworth JA 1992. The effect of repeated doses of ivermectin on adult female Onchocerca volvulus in Sierra Leone. *Trop Med Parasitol* 43(4):256-262.
66. Ismail MM, Weil GJ, Jayasinghe KSA, Premaratne UN, Abeyewickreme W, Rajaratnam HN, Sheriff MHR, Perera CS, Dissanaik AS 1996. Prolonged clearance of microfilaraemia in patients with bancroftian filariasis after multiple high doses of ivermectin or diethylcarbamazine. *Transactions of the Royal Society of Tropical Medicine and Hygiene* 90(6):684-688.
67. Campbell WC. 2012. Ivermectin and Abamectin. ed.: Springer.
68. Valadas E, Gomes A, Sutre A, Brilha S, Wete A, Hanscheid T, Antunes F 2013. Tuberculosis with malaria or HIV co-infection in a large hospital in Luanda, Angola. *Journal of infection in developing countries* 7(3):269-272.
69. Nyamogoba HD, Mbuthia G, Mining S, Kikui G, Biegon R, Mpoke S, Menya D, Waiyaki PG 2012. HIV co-infection with tuberculous and non-tuberculous mycobacteria in western Kenya: challenges in the diagnosis and management. *African health sciences* 12(3):305-311.
70. Tshikuka Mulumba JG, Atua Matindii B, Kilauzi AL, Mengema B, Mafuta J, Eloko Eya Matangelo G, Mukongo Bulaimu-Lukeba A, Jerry IL 2012. Severity of outcomes associated to types of HIV coinfection with TB and malaria in a setting where the three pandemics overlap. *Journal of community health* 37(6):1234-1238.

1  
2  
3  
4  
5  
6  
7  
8  
9  
10  
11  
12  
13  
14  
15  
16  
17  
18  
19  
20  
21  
22  
23  
24  
25  
26  
27  
28  
29  
30  
31  
32  
33  
34  
35  
36  
37  
38  
39  
40  
41  
42  
43  
44  
45  
46  
47  
48  
49  
50  
51  
52  
53  
54  
55  
56  
57  
58  
59  
60

785 71. Klotz U, Ogbuokiri JE, Okonkwo PO 1990. Ivermectin binds avidly to plasma  
786 proteins. *European journal of clinical pharmacology* 39(6):607-608.  
787 72. Crump A 2017. Ivermectin: enigmatic multifaceted ‘wonder’ drug continues to  
788 surprise and exceed expectations. *The Journal of Antibiotics* 70(5):495-505.  
789 73. Campbell W 1985. Ivermectin: an update. *Parasitology Today* 1(1):10-16.  
790 74. DrugBank. Ivermectin. ed.  
791 75. Borrmann S, Sallas WM, Machevo S, Gonzalez R, Bjorkman A, Martensson A,  
792 Hamel M, Juma E, Peshu J, Ogutu B, Djimde A, D'Alessandro U, Marrast AC, Lefevre G,  
793 Kern SE 2010. The effect of food consumption on lumefantrine bioavailability in African  
794 children receiving artemether-lumefantrine crushed or dispersible tablets (Coartem) for acute  
795 uncomplicated *Plasmodium falciparum* malaria. *Trop Med Int Health* 15(4):434-441.  
796 76. Ezzet F, van Vugt M, Nosten F, Looareesuwan S, White NJ 2000. Pharmacokinetics  
797 and pharmacodynamics of lumefantrine (benflumetol) in acute *falciparum* malaria.  
798 *Antimicrob Agents Chemother* 44(3):697-704.

799  
800

## LIST OF FIGURES

### Figure 1: PBPK workflow model

A 6-step workflow model was implemented. Clinical studies utilised for Step 1 ivermectin compound model development and validation are listed in the figure and fully described in Section 2.1.

### Figure 2: The simulated plasma concentration-time profile of ivermectin in adults

Ivermectin was dosed based on the reported clinical studies (see Methods section for details) to healthy volunteer adults. Mean observed plasma concentrations are represented by the open circles, with error bars indicating standard deviations on either the reported concentrations (vertical) or reported  $t_{\max}$  (horizontal). Solid lines represent predicted mean plasma concentration with dashed lines indicating 5<sup>th</sup> and 95<sup>th</sup> percentiles. For the study by Na-Bangchang *et al.* (2006), red circles indicate data extracted from complete plasma concentrations profile 'lines' for individual subjects rather than discrete time-points.

### Figure 3: The simulated impact of dose escalation on ivermectin plasma concentration-time profiles in healthy volunteer adult subjects

Ivermectin was dosed as: (A) single oral doses of 0.15-0.60 mg/kg; (B) a single 2 mg/kg oral dose; (C) a single daily oral dose of 0.15-0.60 mg/kg for three days; (D) twice daily 0.6 mg/kg oral dose for three days; (E) once daily oral dose of 0.60 mg/kg for five days; (F) twice daily oral doses of 0.60 mg/kg for five days. For all simulations, 100 subjects were simulated with age ranges of 20-50 years. Solid lines represent predicted mean plasma concentrations with dashed lines indicated 5<sup>th</sup> and 95<sup>th</sup> percentiles of the lowest and highest doses, where relevant. The dashed horizontal lines indicated the proposed therapeutic window based on the reported LC50 of 16 ng/mL (lower line) and upper (maximum) concentration simulated from the 2-mg single dose study (435.20 ng/mL).

**Figure 4: The simulated impact of dose escalation on ivermectin plasma concentration-time profiles in healthy volunteer paediatric subjects**

Ivermectin was dosed as (A) single oral doses of 0.15-0.60 mg/kg; (B) a single 2 mg/kg oral dose; (C) single daily oral doses of 0.15-0.60 mg/kg for three days; (D) twice daily oral doses of 0.60 mg/kg for three days; (E) daily oral doses of 0.60 mg/kg for 5 days; (F) twice daily oral doses of 0.60 mg/kg for 5 days. For all simulations 100 subjects were simulated with age ranges of 3-5 years. Solid lines represent predicted mean plasma concentrations with dashed lines indicated 5<sup>th</sup> and 95<sup>th</sup> percentiles of the lowest and highest doses, where relevant. The dashed horizontal lines indicated the proposed therapeutic window based on the reported LC50 of 16 ng/mL (lower line) and upper (maximum) concentration simulated from the 2-mg single dose study (516.91 ng/mL).

**Figure 5: The simulated impact of an efavirenz-mediated drug-drug interaction on ivermectin plasma concentration-time profiles in healthy volunteer adult subjects**

Efavirenz was dosed as single daily 600 mg oral doses throughout the simulation duration with ivermectin dosed on day 13 onwards, under increasing doses from 0.15 mg/kg to 2 mg/kg as: (A) once daily doses; (B) 1 mg/kg and 2 mg/kg as twice daily doses for three days; (C) 1 mg/kg and 2 mg/kg as twice daily doses for five days. For all simulations 100 subjects were simulated with data representing ivermectin plasma concentration profiles in the presence of efavirenz. Solid lines represent predicted mean plasma concentrations with shaded areas indicating 5<sup>th</sup> and 95<sup>th</sup> percentiles of the lowest and highest doses respectively. The dashed horizontal lines indicated the proposed therapeutic window based on the reported LC50 of 16 ng/mL (lower line) and upper (maximum) concentration simulated from the 2-mg single dose study (435.20 ng/mL).

**Figure 6: The simulated impact of an efavirenz-mediated drug-drug interaction on ivermectin plasma concentration-time profiles in healthy volunteer paediatric subjects**

Efavirenz was dosed as single daily 250 mg (15-20 kg) or 300 mg (20-25 kg) oral doses throughout the simulation duration with ivermectin dosed on day 13 onwards under increasing doses from 0.60 mg/kg to 2 mg/kg as: (A) once daily doses; (B) 1 mg/kg and 2 mg/kg as twice daily doses for three days; (C) 1 mg/kg and 2 mg/kg as twice daily doses for

five days. For all simulations, 100 subjects were simulated with data representing ivermectin plasma concentration profiles in the presence of efavirenz. Data for both the 250mg and 300 mg efavirenz dose were pooled, and the mean presented, with simulations containing at least 50 subjects within each dosing band. Solid lines represent predicted mean plasma concentrations with shaded regions indicating 5<sup>th</sup> and 95<sup>th</sup> percentiles of the lowest and highest doses respectively. The dashed horizontal lines indicated the proposed therapeutic window based on the reported LC50 of 16 ng/mL (lower line) and upper (maximum) concentration simulated from the 2-mg single dose study (516.91 ng/mL).

**Figure 7: Simulated ivermectin plasma concentration in adult and paediatric malaria population group**

Ivermectin was dosed at 0.60 mg/kg or 1 mg/kg to adults (20-50 years) and paediatrics (3-5 years) under 3-day dosing (black and red) or 5-day dosing (green). The healthy volunteer population group (Caucasian) was used as a default population group with the Thailand population group created with appropriate age-weight distributions and changes in blood biochemistry to mimic a malaria population group. For all simulations, 100 subjects were simulated. Solid lines represent predicted mean plasma concentrations with shaded regions indicating 5<sup>th</sup> and 95<sup>th</sup> percentiles of the Thailand malaria and Caucasian populations, respectively. The dashed horizontal lines indicated the proposed therapeutic window based on the reported LC50 of 16 ng/mL (lower line) and upper (maximum) concentration simulated from the 2-mg single dose study.

LIST OF TABLES

Table 1. Final optimised ivermectin parameters for multi-dose simulations

Parameters	Value	Notes
Compound type	Neutral	
Molecular weight (g/mol)	875.1 <sup>1</sup>	
Log P	5.8 <sup>2</sup>	
fu	0.068 <sup>3</sup>	
pKa 1	-	
pKa 2	-	
B/P	3.62	Predicted by Simcyp Prediction Toolbox
Vss (L/kg)	1.34	Final optimised using a minimal PBPK model with a SAC <sup>a</sup>
SAC (L/kg)	0.179	
k <sub>in</sub> (h <sup>-1</sup> )	0.1751	
k <sub>out</sub> (h <sup>-1</sup> )	0.0336	
Papp (x10 <sup>-6</sup> cm/s)	7.6 <sup>4</sup>	
CL <sub>int</sub> <sub>P-glycoprotein</sub> (μL/min)	2.5 <sup>b</sup>	
RAF	0.1 <sup>b</sup>	
k <sub>a</sub> (h <sup>-1</sup> )	0.38	Estimated from Peff
fa	0.69	Estimated from Peff
CL <sub>po</sub> (L/h)	21.25 <sup>c</sup>	Mean from literature
CL <sub>int</sub> <sub>3A4</sub> (μL/min/pmol)	0.28 <sup>c</sup>	Final optimised
Absorption model	ADAM	
Distribution model	Minimal	

<sup>a</sup> Parameter estimated using a minimal PBPK model with a single adjusting compartment (SAC). <sup>b</sup> The contribution of active efflux to ivermectin intestinal absorption was assumed to be similar to that of the reported value for digoxin <sup>5</sup>, with RAF empirically optimised through a sensitivity analysis (see supplementary materials). <sup>c</sup> CL<sub>int</sub><sub>CYP</sub> was based on a retrograde calculation, described in Step 1, with fa fixed at 0.56 and F<sub>G</sub> assumed = 1. Final estimates were obtained through parameter estimation assuming an fmcyp of 1 for CYP3A4.

Log P: octanol/water partition coefficient;  $f_u$ : unbound fraction; B/P: blood-to-plasma ratio;  $V_{ss}$ : steady state volume of distribution;  $k_a$ : absorption rate constant;  $f_a$ : fraction dose absorbed;  $CL_{po}$ : oral clearance;  $CL_{int}$ : *in vitro* intrinsic clearance for active efflux (P-glycoprotein) or metabolism (3A4);  $F_G$ : fraction of drug escaping the gut enterocyte intact; RAF: relative activity factor.

For Peer Review

Table 2: Summary of predicted and observed pharmacokinetic parameters of ivermectin used in the validation

Study		C <sub>max</sub> (ng/mL)		t <sub>max</sub> (h)		AUC <sub>0-inf</sub> or AUC <sub>0-time</sub> (ng/mL.h)	
Name and Dose		<i>Predicted</i>	<i>Observed</i>	<i>Predicted</i>	<i>Observed</i>	<i>Predicted</i>	<i>Observed</i>
Guzzo: 30mg <sup>6</sup>	<i>Day 1</i>	77.82 ± 31.12	84.8 ± 42.7	3.52 ± 0.4	4.3 ± 1	1629.23 ± 650.58	1724.3 ± 830.5
	<i>Day 7</i>	99.85 ± 58.25	87.0 ± 42.2	3.79 ± 1.2	4.2 ± 0.9	3239.82 ± 1356.66	2819.4 ± 1691.2
Guzzo: 60mg <sup>6</sup>	<i>Day 1</i>	114.23 ± 102.99	165.2 ± 95.6	3.11 ± 0.8	3.6 ± 0.9	2429.63 ± 1311.74	2984 ± 1530.1
	<i>Day 7</i>	162.87 ± 143.13	186.2 ± 130.8	3.40 ± 1.2	4.0 ± 1.1	6187.15 ± 3982.52	6061.7 ± 4243.7
Guzzo: 90 mg <sup>6</sup>	<i>Single</i>	151.63 ± 95.26	158.1 ± 87.6	4.11 ± 0.85	4.9 ± 1.8	3814.24 ± 1324.07	2910.2 ± 1801.9
Guzzo: 120 mg <sup>6</sup>	<i>Single</i>	171.33 ± 112.28	247.8 ± 158.9	4.18 ± 0.89	4.2 ± 0.9	5124.61 ± 1498.92	4547.7 ± 2402.9
Edwards: 12 mg <sup>7</sup>	<i>Single</i>	40.29 ± 13.36	46 ± 20	3.40 ± 0.35	3.6 ± 0.7	588.71 ± 211.19	885 ± 389
Baraka: 0.15 µg/kg <sup>8</sup>	<i>Single</i>	49.62 ± 11.36	54.4 ± 12.2	3.40 ± 0.31	4.9 ± 1.5	797.31 ± 157.33	3180 ± 1390
Na-Bangchang: 0.2 µg/kg <sup>9</sup>	<i>Single</i>	54.01 ± 14.51	-	3.70 ± 0.3	-	1609.22 ± 578.24	-
Njoo: 0.15 µg/mL <sup>10</sup>	<i>Single</i>	39.94 ± 9.31	-	3.67 ± 0.29	-	1229.27 ± 436.68	-
Okonkwo: 0.15 µg/mL <sup>11</sup>	<i>Single</i>	40.45 ± 15.62	38.2 ± 16.15	3.73 ± 0.58	4.7 ± 1.49	862.12 ± 277.27	1545.3 ± 537.4

Data represent mean ± SD; AUC<sub>0-time</sub> calculated for studies by Okonkwo<sup>11</sup> and Edwards<sup>7</sup>.

AUC<sub>0-time</sub>: AUC calculated for the study period only; AUC<sub>0-inf</sub>: AUC calculated from the start of the study and extrapolated to infinity.



**Table 3: Simulated pharmacokinetic parameters of ivermectin under dose escalation in healthy adult subjects**

Duration	Dose (mg/kg)	C <sub>max</sub> (ng/mL)	t <sub>max</sub> (h)	AUC <sub>final dose-t</sub> (ng/mL.h)	Time above LC50 (h)
<i>Single</i>	0.15	35.47 ± 8.77	3.41 ± 0.36	342.58 ± 89.93	10.4
	0.3	60.52 ± 15.12	3.49 ± 0.39	595.75 ± 164.26	15.8
	0.6	95.86 ± 31.72	3.55 ± 0.40	960.29 ± 335.66	23.2
	2	178.38 ± 95.98	3.70 ± 0.42	1779.92 ± 890.56	> 24
<i>3 Days</i>	0.15	41.11 ± 10.48	3.40 ± 0.37	1255.36 ± 522.29	32.2
	0.3	70.80 ± 20.03	3.47 ± 0.38	2213.06 ± 1003.6	86.2
	0.6	113.11 ± 39.54	3.49 ± 0.37	3581.99 ± 1777.58	152.9
	0.6 BD	151.51 ± 66.22	3.29 ± 0.34	6292.28 ± 3659.18	178.2
<i>5 Days</i>	0.6	124.54 ± 53.19	3.51 ± 0.37	4543.99 ± 2513.48	182.3
	0.6 BD	174.41 ± 73.69	3.30 ± 0.35	8024.87 ± 4667.20	257.1

Data represents median ± SD. n=100. For 3- and 5-day simulations, AUC was calculated from the final dosing period to the end of the study period. Time above LC50 (16 ng/mL) was calculated from the median line of each simulation. BD: twice daily.

**Table 4: Simulated pharmacokinetic parameters of ivermectin under dose escalation in healthy paediatric subjects**

Duration	Dose (mg/kg)	C <sub>max</sub> (ng/mL)	t <sub>max</sub> (h)	AUC <sub>final dose-t</sub> (ng/mL.h)	Time above LC50 (h)
Single	0.15	42.92 ± 8.91	3.60 ± 0.46	394.10 ± 87.71	10.1
	0.3	81.41 ± 19.85	3.67 ± 0.56	763.97 ± 202.29	14.6
	0.6	145.07 ± 41.43	3.75 ± 0.59	1397.10 ± 444.39	23.9
	2	348.40 ± 148.95	3.98 ± 0.75	3423.15 ± 1506.71	> 24
3 Days	0.15	51.02 ± 10.31	3.58 ± 0.45	1454.62 ± 600.10	37.1
	0.3	97.39 ± 23.83	3.64 ± 0.52	2858.04 ± 1252.65	88.1
	0.6	174.85 ± 51.30	3.72 ± 0.58	5340.55 ± 2593.37	151.2
	0.6 BD	225.54 ± 80.71	3.56 ± 0.54	9109.37 ± 4790.91	214.5
5 Days	0.6	206.22 ± 62.35	3.58 ± 0.51	7278.17 ± 3843.94	234.5
	0.6 BD	263.82 ± 98.72	3.48 ± 0.48	11712.94 ± 6438.28	290.1

Data represents median ± SD. *n*=100. For 3- and 5-day simulations, AUC was calculated from the final dosing period to the end of the study period. Time above LC50 (16 ng/mL) was calculated from the median line of each simulation. BD: twice daily.

**Table 5: Simulated pharmacokinetic parameters of ivermectin in the presence of an efavirenz-mediated drug-drug interactions in healthy adult subjects**

Duration	Dose	C <sub>max</sub>	t <sub>max</sub>	AUC <sub>final dose-t</sub>	AUC Ratio	Cmax Ratio	Time above LC50
	(mg/kg)	(ng/mL)	(h)	(ng/mL.h)			(h)
3 Days	0.15	23.61 ± 7.92	2.77 ± 0.38	264.23 ± 115.69	0.28 ± 0.06	0.48 ± 0.10	9.3
	0.3	40.78 ± 14.53	2.78 ± 0.38	462.28 ± 203.15	0.28 ± 0.06	0.48 ± 0.10	19.7
	0.6	65.40 ± 25.89	2.83 ± 0.39	740.13 ± 325.21	0.28 ± 0.06	0.48 ± 0.10	24.2
	1	82.12 ± 38.98	2.87 ± 0.37	1052.84 ± 476.63	0.28 ± 0.06	0.48 ± 0.10	30.8
	2	120.39 ± 61.70	2.92 ± 0.37	1360.83 ± 645.68	0.28 ± 0.06	0.48 ± 0.10	47.5
	1 BD	99.72 ± 48.73	2.78 ± 0.22	1533.18 ± 810.62	0.23 ± 0.06	0.42 ± 0.08	77.3
	2 BD	136.16 ± 72.64	2.89 ± 0.36	1879.75 ± 973.82	0.25 ± 0.06	0.42 ± 0.08	91.2
5 Days	1 BD	106.4 ± 51.37	2.80 ± 0.31	1623.55 ± 865.22	0.23 ± 0.06	0.40 ± 0.07	138.8
	2 BD	145.67 ± 76.98	2.84 ± 0.32	2347.87 ± 1217.91	0.21 ± 0.06	0.39 ± 0.07	144.7

Data represent median ± SD in the presence of efavirenz. n=100.

For 3- and 5-day simulations, AUC<sub>final dose-t</sub> was calculated from the final dosing period to the end of the study period. Time above LC50 (16 ng/mL) was calculated from the median line of each simulation. BD: twice daily.

1  
2  
3  
4  
5  
6  
7  
8  
9  
10  
11  
12  
13  
14  
15  
16  
17  
18  
19  
20  
21  
22  
23  
24  
25  
26  
27  
28  
29  
30  
31  
32  
33  
34  
35  
36  
37  
38  
39  
40  
41  
42  
43  
44  
45  
46  
47

**Table 6: Simulated pharmacokinetic parameters of ivermectin in the presence of an efavirenz-mediated drug-drug interaction in healthy paediatric subjects**

Duration	Dose	C <sub>max</sub>	t <sub>max</sub>	AUC <sub>final dose-t</sub>	AUC Ratio	C <sub>max</sub> Ratio	Time above LC50
	(mg/kg)	(ng/mL)	(h)	(ng/mL.h)			(h)
3 Days	0.6	98.25 ± 55.72	2.88 ± 0.47	909.93 ± 579.05	0.21 ± 0.10	0.43 ± 0.13	27.8
	1	159.28 ± 92.85	3.00 ± 0.56	1799.69 ± 987.56	0.21 ± 0.09	0.43 ± 0.12	30.9
	2	240.45 ± 150.97	3.08 ± 0.59	2225.53 ± 1503.45	0.21 ± 0.09	0.43 ± 0.12	30.9
	1 BD	155.06 ± 90.31	2.98 ± 0.55	1754.32 ± 1144.67	0.19 ± 0.09	0.37 ± 0.12	81.2
5 Days	2 BD	257.42 ± 162.43	3.07 ± 0.64	2812.20 ± 1929.57	0.19 ± 0.09	0.38 ± 0.12	104.2
	1 BD	176.32 ± 98.71	3.06 ± 0.46	2071.25 ± 1347.96	0.20 ± 0.09	0.36 ± 0.12	141.2
	2 BD	274.51 ± 165.31	3.11 ± 0.58	3114.23 ± 2006.82	0.20 ± 0.09	0.36 ± 0.12	142.1

Data represent median ± SD in the presence of efavirenz. n=100.

For 3- and 5-day simulations, AUC<sub>final dose-t</sub> was calculated from the final dosing period to the end of the study period. Time above LC50 (16 ng/mL) was calculated from the median line of each simulation. BD: twice daily.

## REFERENCES

1. NCBI. 2017. PubChem Compound Database. ed.
2. DrugBank. Ivermectin. ed.
3. Klotz U, Ogbuokiri JE, Okonkwo PO 1990. Ivermectin binds avidly to plasma proteins. *European journal of clinical pharmacology* 39(6):607-608.
4. Kigen G, Edwards G 2017. Drug-transporter mediated interactions between anthelmintic and antiretroviral drugs across the Caco-2 cell monolayers. *BMC Pharmacology and Toxicology* 18(1):20.
5. Schinkel AH, Wagenaar E, van Deemter L, Mol CA, Borst P 1995. Absence of the *mdr1a* P-Glycoprotein in mice affects tissue distribution and pharmacokinetics of dexamethasone, digoxin, and cyclosporin A. *Journal of Clinical Investigation* 96(4):1698-1705.
6. Guzzo CA, Furtek CI, Porras AG, Chen C, Tipping R, Clineschmidt CM, Sciberras DG, Hsieh JY, Lasseter KC 2002. Safety, tolerability, and pharmacokinetics of escalating high doses of ivermectin in healthy adult subjects. *Journal of clinical pharmacology* 42(10):1122-1133.
7. Edwards G, Dingsdale A, Helsby N, Orme ML, Breckenridge AM 1988. The relative systemic availability of ivermectin after administration as capsule, tablet, and oral solution. *European journal of clinical pharmacology* 35(6):681-684.
8. Baraka OZ, Mahmoud BM, Marschke CK, Geary TG, Homeida MMA, Williams JF 1996. Ivermectin distribution in the plasma and tissues of patients infected with *Onchocerca volvulus*. *European journal of clinical pharmacology* 50(5):407-410.
9. Na-Bangchang K, Banmairuroi V, Choemung A 2006. High-performance liquid chromatographic method for the determination of ivermectin in plasma. *Southeast Asian J Trop Med Public Health* 37(5):848-858.
10. Njoo FL, Beek WMJ, Keukens HJ, Van Wilgenburg H, Oosting J, Stilma JS, Kijlstra A 1995. Ivermectin Detection in Serum of Onchocerciasis Patients: Relationship to Adverse Reactions. *The American Journal of Tropical Medicine and Hygiene* 52(1):94-97.
11. Okonkwo PO, Ogbuokiri JE, Ofoegbu E, Klotz U 1993. Protein binding and ivermectin estimations in patients with onchocerciasis. *Clinical Pharmacology & Therapeutics* 53(4):426-430.

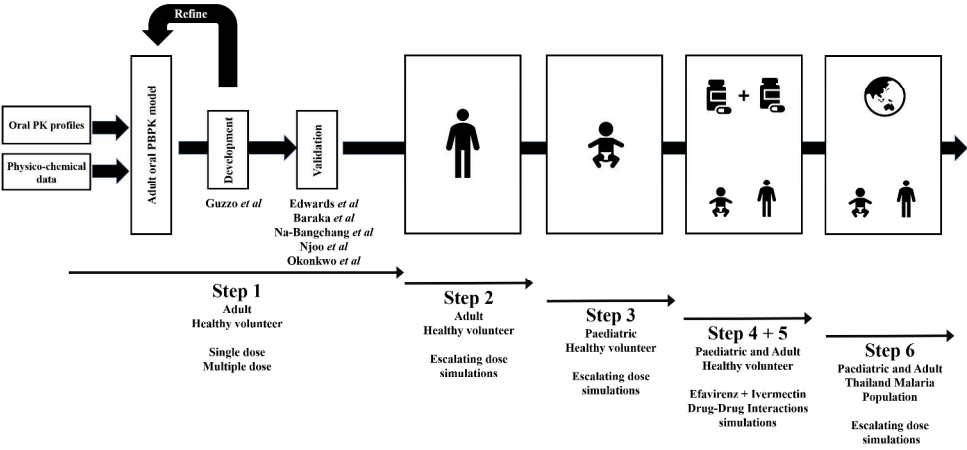
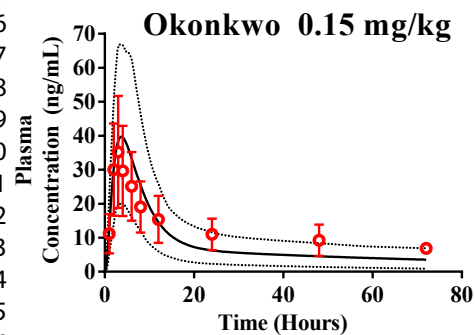
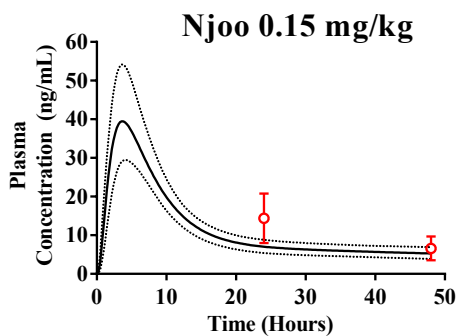
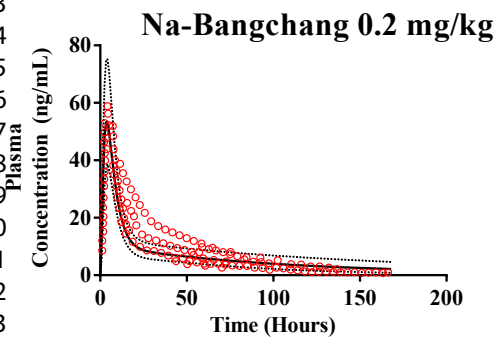
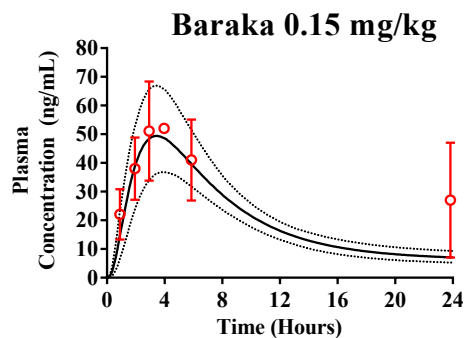
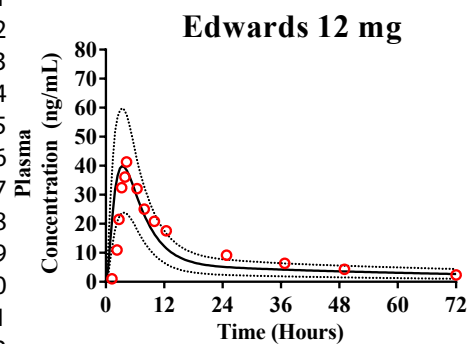
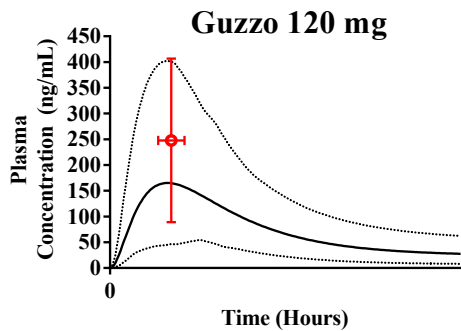
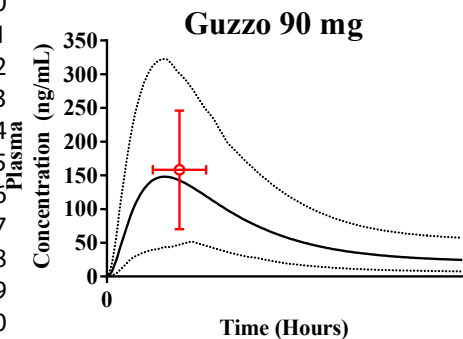
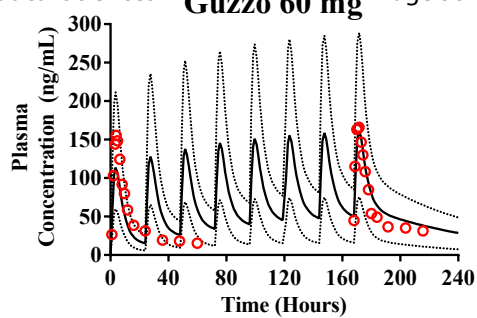
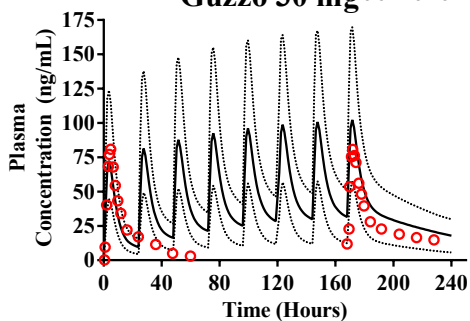


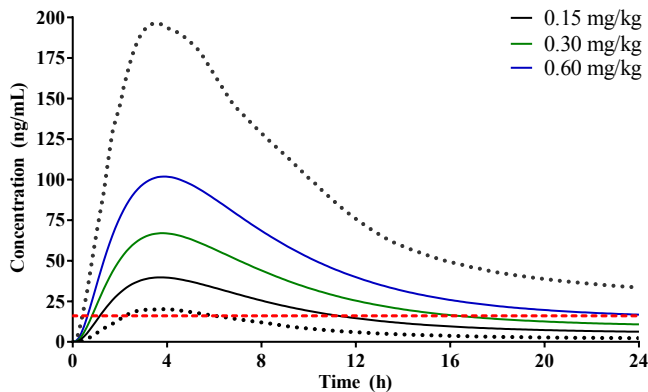
Figure 1

931x448mm (96 x 96 DPI)

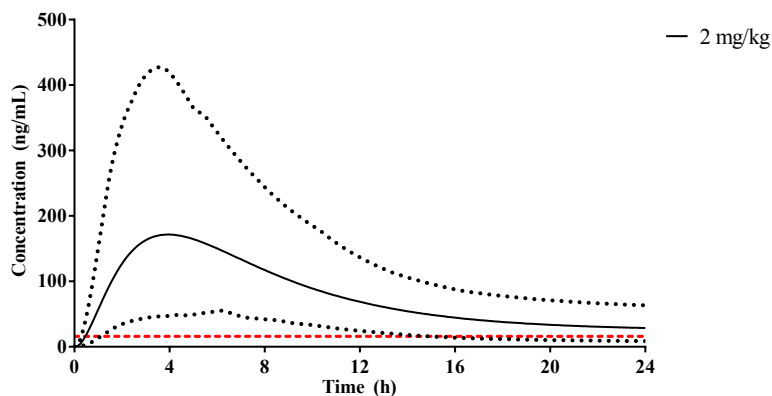




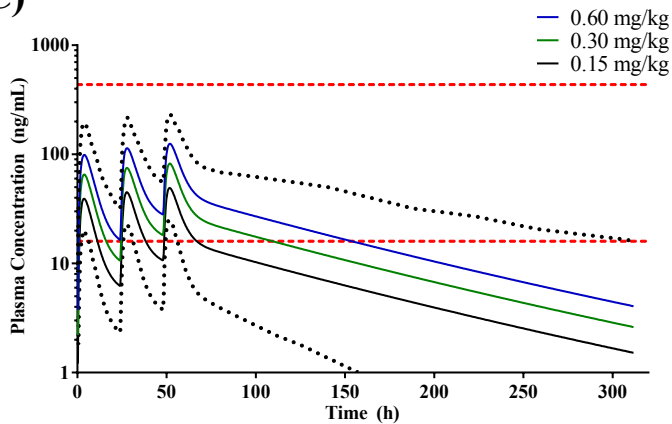
(A)



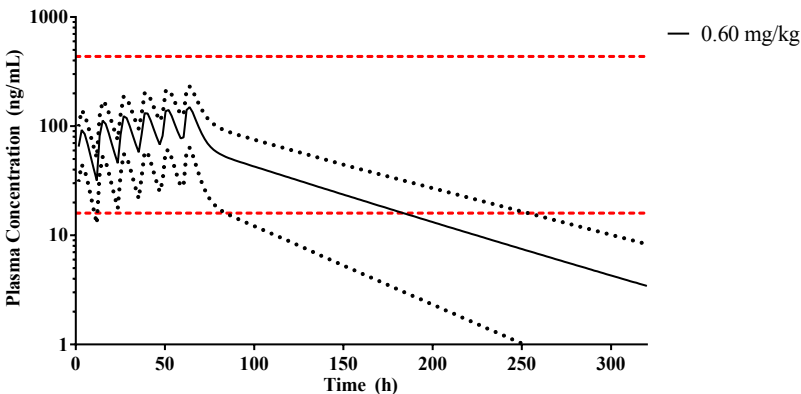
(B)



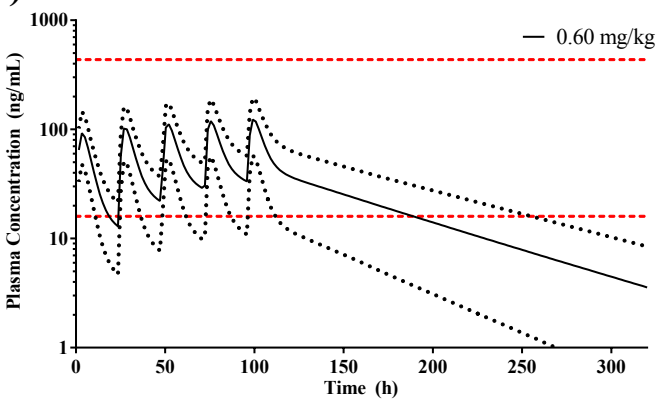
(C)



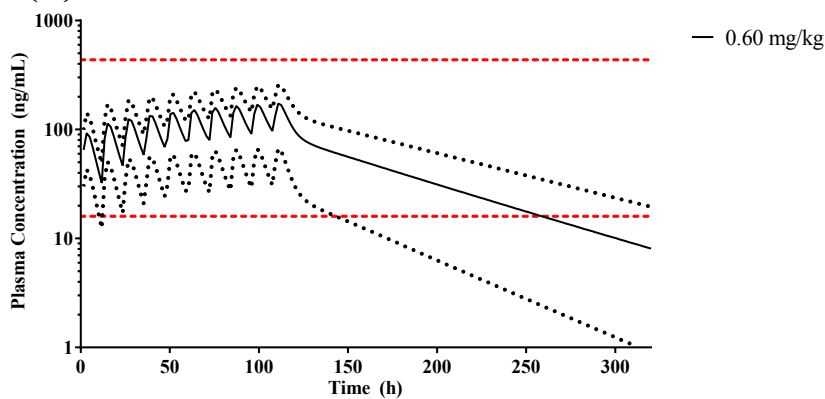
(D)



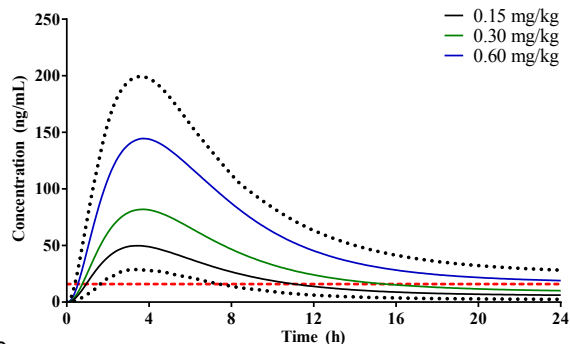
(E)



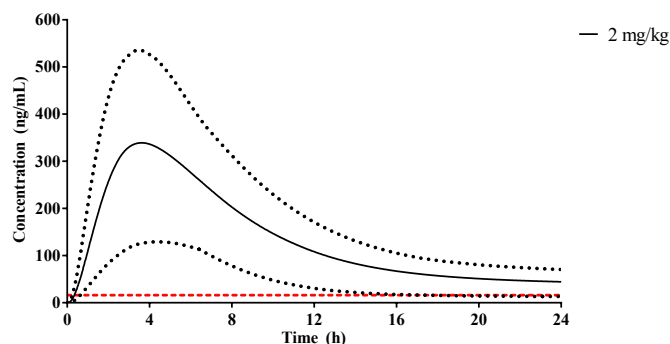
(F)



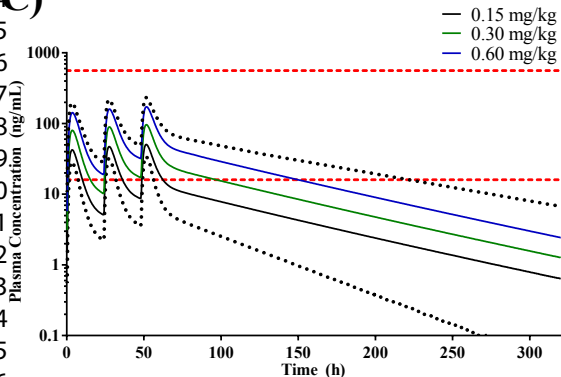
(A)



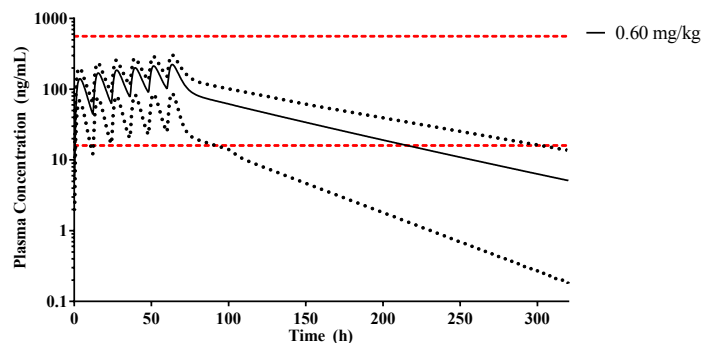
(B)



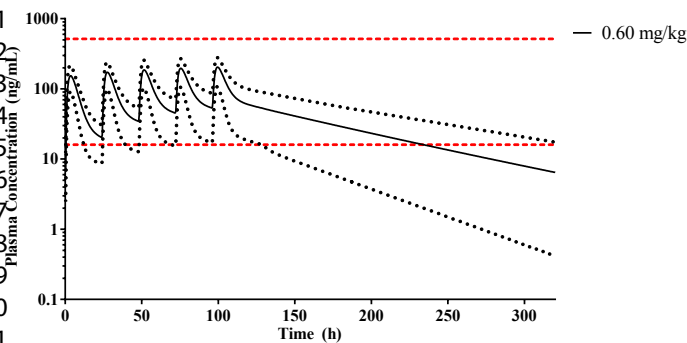
(C)



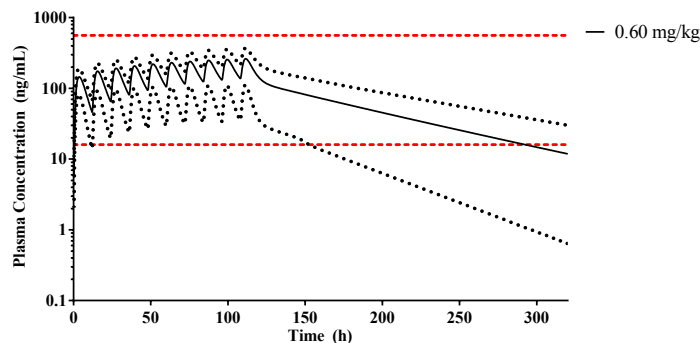
(D)



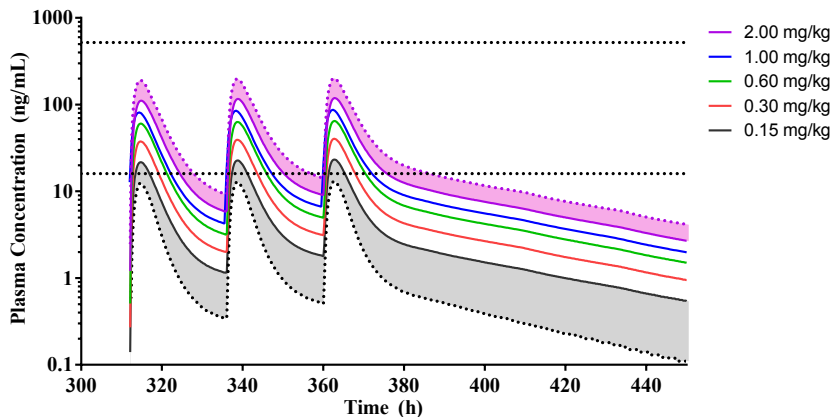
(E)



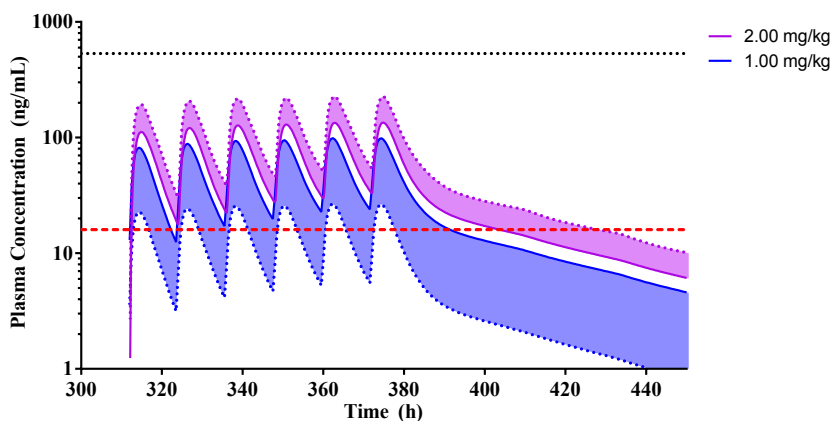
(F)



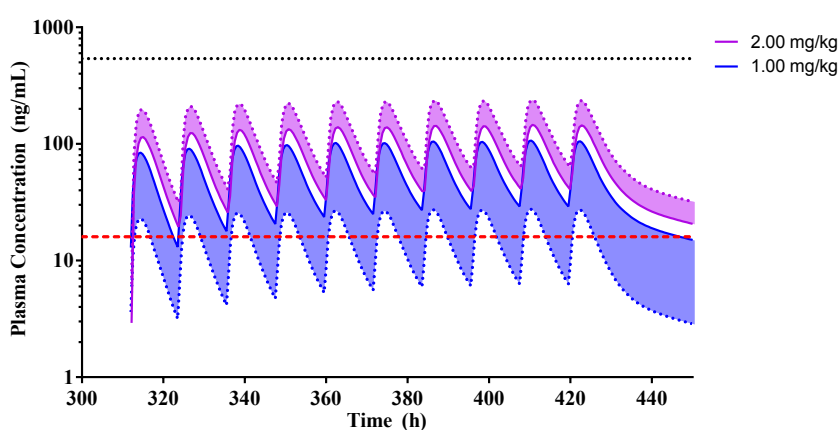
(A)



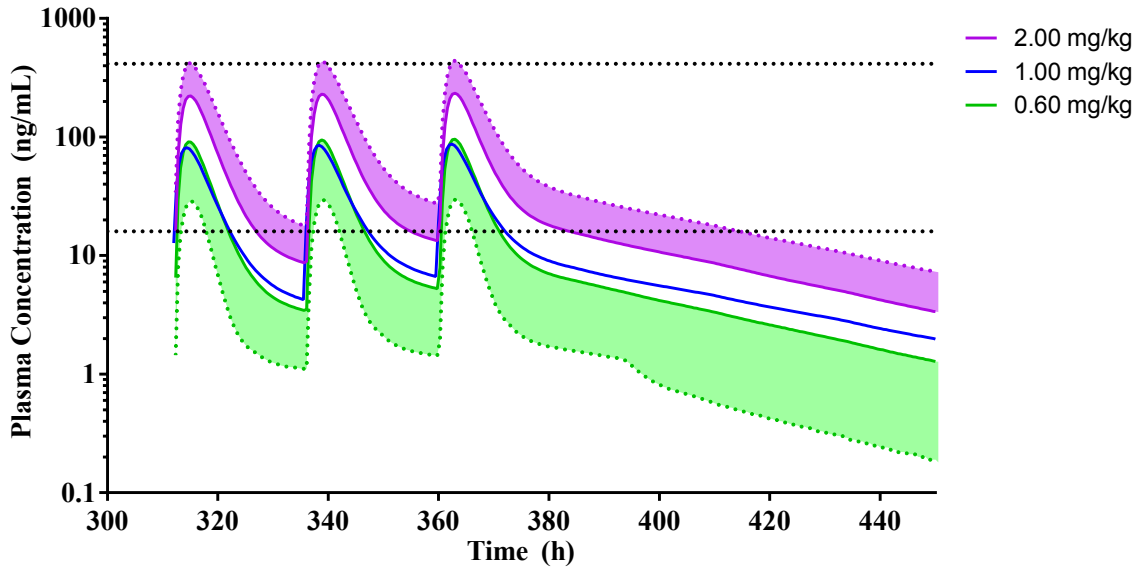
(B)



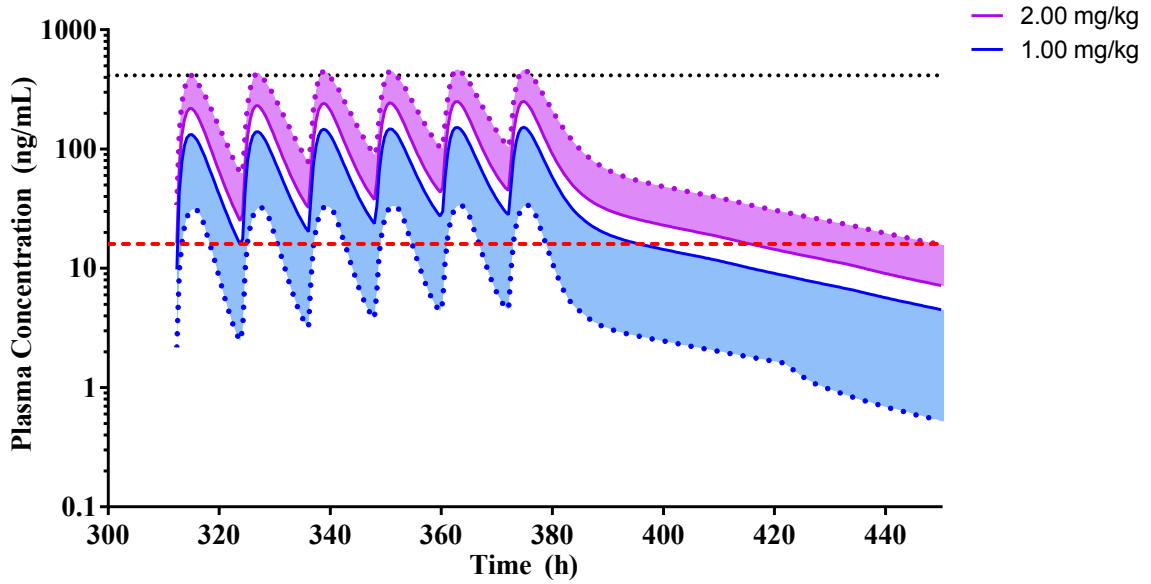
(C)



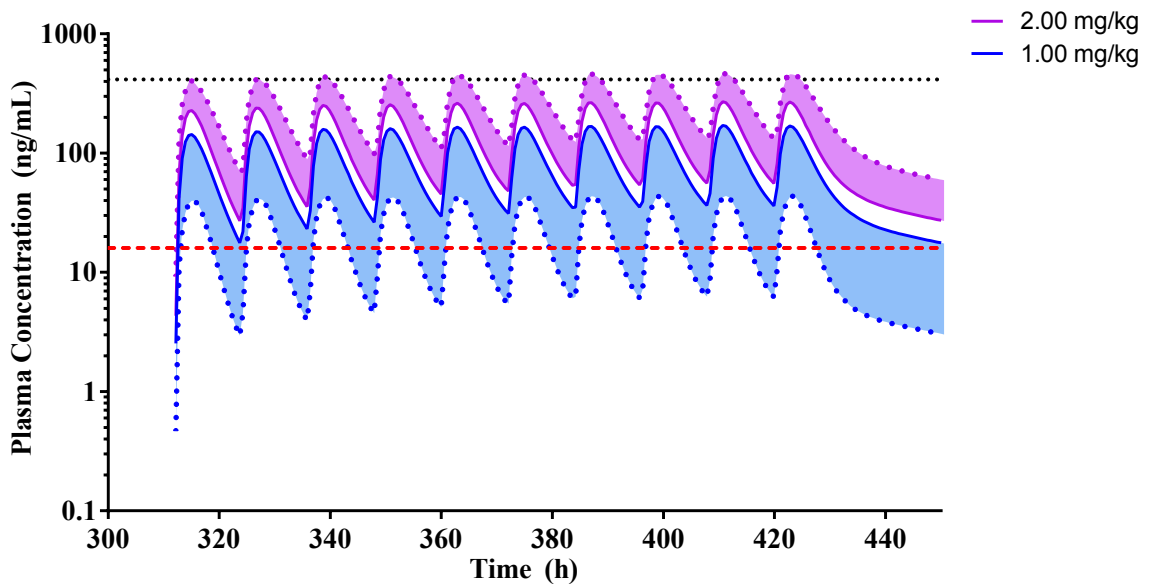
(A)



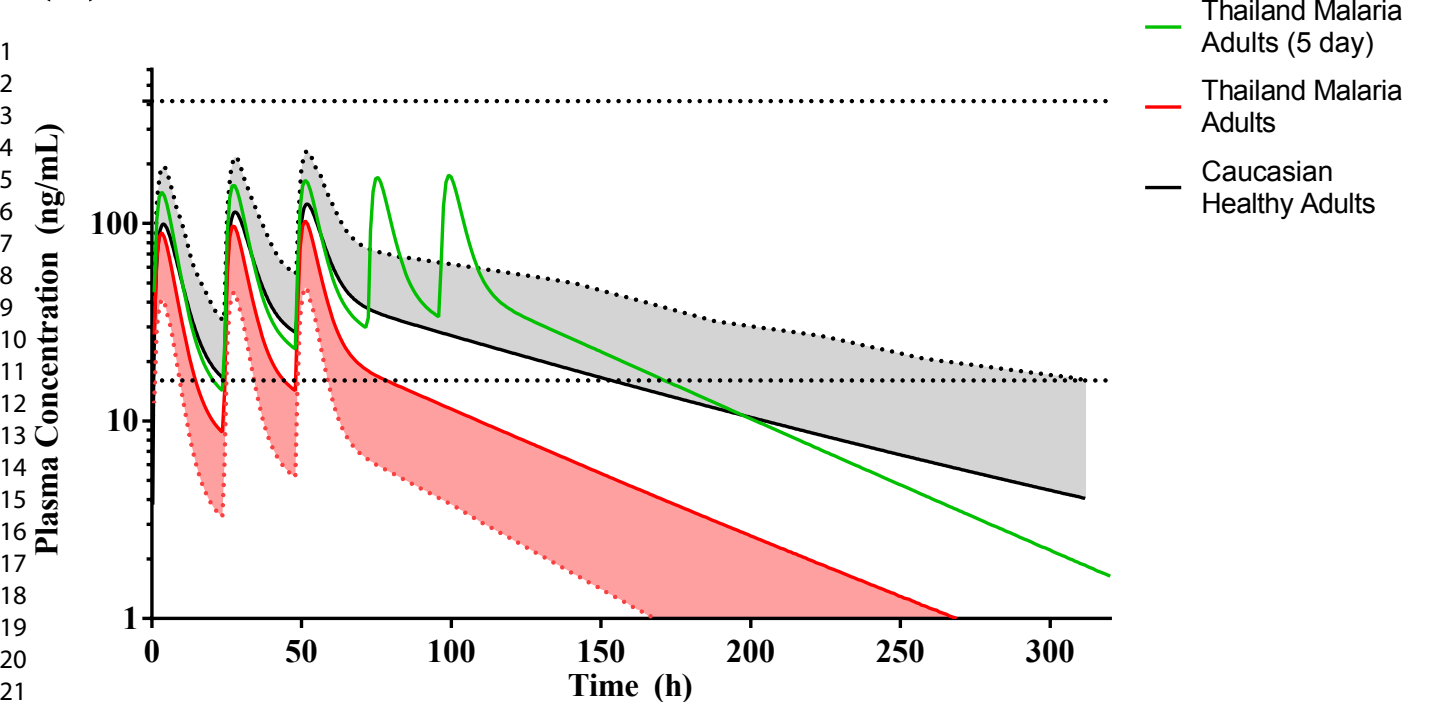
(B)



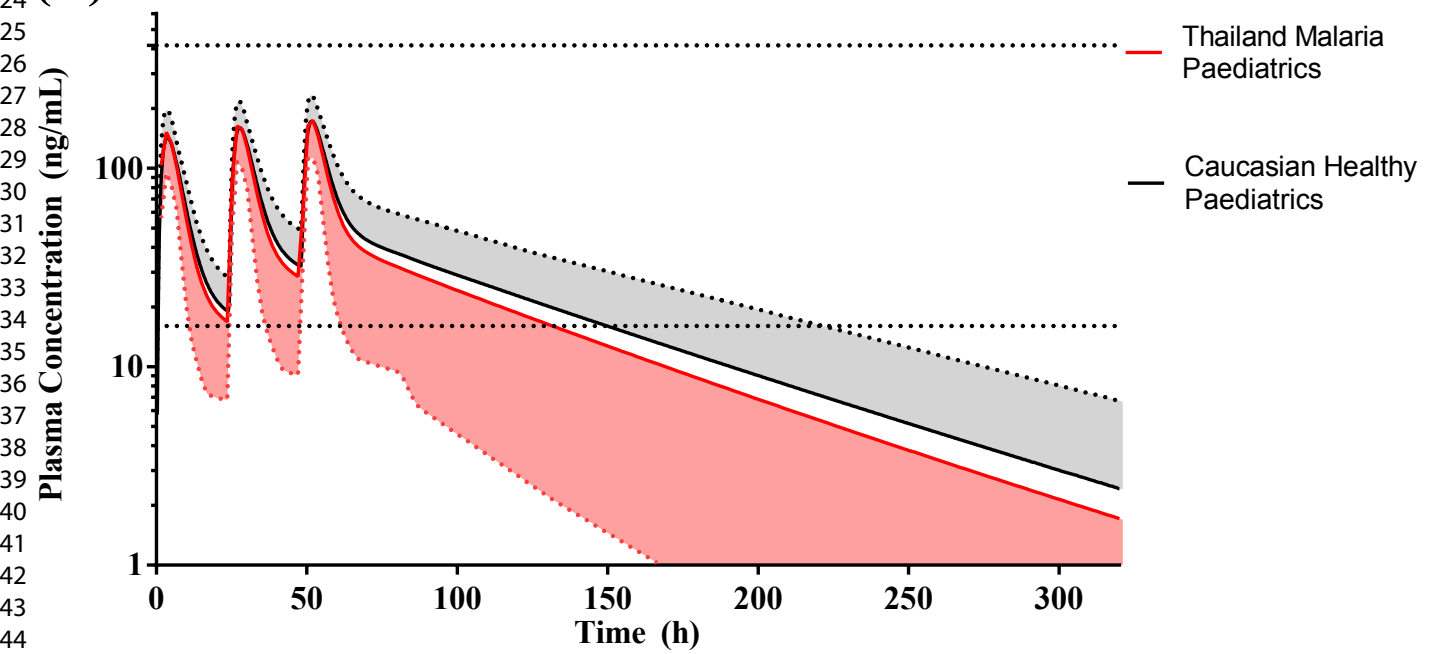
(C)



(A)



(B)



## Supplementary materials

### Section 1: Model development

#### *Steady-state volume of distribution (Vss)*

To recover the shape of the distribution and elimination phases of the plasma-concentration time profiles, estimation of the steady-state volume of distribution (Vss) was determined from published clinical data through parameter estimation with observed plasma concentration-time profiles using a weighted least square algorithm with a Nelder-Mead minimisation method, to yield a Vss of 1.343 L/kg using a minimal PBPK model. Estimation of the single adjustment compartments (SAC) was 0.179 L/kg with inter-compartmental transfer constants  $k_{in}$  and  $k_{out}$  of  $0.1751\text{ h}^{-1}$  and  $0.0336\text{ h}^{-1}$ .

#### *Metabolic Intrinsic clearance (CLint)*

The ready availability of *in-vitro* metabolic intrinsic clearance data is limited for ivermectin. However, it has been identified that CYP3A4 is the major metabolic pathway<sup>1</sup>. It was therefore assumed that the major pathway would be attributed to CYP3A4 with an intrinsic clearance (CLint<sub>3A4</sub>) estimated using the Simcyp retrograde calculator using a fixed CL<sub>oral</sub> of 21.25 L/h, the mean of 5 reported individual CL<sub>oral</sub><sup>2,3</sup> (and assuming  $fa \sim 0.56$ <sup>4</sup>), with CYP3A4 allocated 100 % of the total clearance. The final predicted CLint<sub>3A4</sub> was 0.28  $\mu\text{L}/\text{min}/\text{pmol}$ . Renal clearance has been reported to be negligible<sup>5</sup> and therefore was not considered within the model.

#### *Passive permeability*

Ivermectin is a low solubility BCS Class II compound, and therefore permeability is thought to be limited. As a result of the lack of a range of published *in-vitro* Caco-2 permeability measurements, a single published study was utilised which reported an *in-vitro* apparent permeability (Papp<sub>AB</sub>) of  $7.6 \times 10^{-6}\text{ cm/s}$ <sup>6</sup>. This was then used in the Simcyp ADAM model to estimate a human jejunum effective permeability (Peff) of  $0.88 \times 10^{-4}\text{ cm/s}$ . Subsequently, this was then used to estimate the absorption rate constant ( $k_a$ ) and fraction dose absorbed ( $fa$ ) using the ADAM model resulting in an initial estimate of  $0.38\text{ h}^{-1}$  and 0.69 for  $k_a$  and  $fa$  respectively. However, attempts to capture an appropriate  $C_{max}$  and  $t_{max}$  for ivermectin ( $\sim 4\text{-}6$  hours)<sup>2,7,8</sup> failed. As ivermectin has also been reported to be a P-glycoprotein substrate<sup>6,9</sup>,

the contribution of active efflux on limiting intestinal absorption and hence delaying  $t_{\max}$  was modelled by the inclusion of an active efflux component into the model.

*Active efflux*

Recently Zhou *et al* (2016)<sup>10</sup> reported the successful development of a Simcyp model for naloxegol. In the absence of *in-vitro* reported kinetic efflux parameters, they utilised the Simcyp default digoxin efflux kinetic parameters as a surrogate for the active efflux of naloxegol. This approach resulted in the successful development of a PBPK model for naloxegol.

As ivermectin P-glycoprotein-specific Michaelis-Menten efflux kinetic parameters are absent in the literature, namely the apparent  $V_{\max}$  (maximum velocity) estimated for the carrier system ( $J_{\max}$ ) and the Michaelis constant ( $K_m$ ), assumptions were made to obtain a reasonable absorption phase profile of ivermectin. We therefore utilised a similar approach as that implemented by Zhou *et al* (2016)<sup>10</sup>, where the default *in-vitro* transporter-mediated intrinsic clearance ( $CL_{\text{intP-glycoprotein}}$ ) value for digoxin ( $2.5 \mu\text{L}/\text{min}$ )<sup>11</sup> along with the default Simcyp validated Relative Activity Factor (RAF) (enables *in-vitro* to *in-vivo* scaling of transport clearances) were used as a surrogate for ivermectin efflux.

Subsequently we conducted a sensitivity analysis to assess this assumption through exploring the impact of changes in  $CL_{\text{intP-glycoprotein}}$  ( $1\text{--}12 \mu\text{L}/\text{min}$ ) and RAF ( $0\text{--}1$ ) on ivermectin  $C_{\max}$  and  $t_{\max}$  (Figure 1), where a 60 mg single oral dose was administered to healthy subjects to mimic the study reported by Guzzo *et al.* (2002)<sup>12</sup>. The impact of increasing  $CL_{\text{intP-glycoprotein}}$  on ivermectin  $C_{\max}$  is significant when  $CL_{\text{intP-glycoprotein}}$  and RAF both increase (Figure 1A), with an equally significant increase in the simulated  $t_{\max}$  (Figure 1B). An empirical assessment of the sensitivity analysis identified an ivermectin RAF of 0.1 would enable a more appropriate estimate of both the ivermectin  $C_{\max}$  and  $t_{\max}$  when compared to Guzzo *et al.* (2002)<sup>12</sup>. When this revised RAF was incorporated into simulations, the model was adequately able to capture the reported  $C_{\max}$  and  $t_{\max}$  for the 60 mg single dose, namely  $165.2 \text{ ng}/\text{ml} \pm 95.6 \text{ ng}/\text{ml}$  and  $3.6 \text{ h} \pm 0.9 \text{ h}$ .

Further, to ensure these parameter values were appropriate for lower doses, these parameters were also used in validation steps using clinical studies ii-v (See Methods Step 1) at body weight based doses of  $0.15 \text{ mg}/\text{kg}\text{--}0.2 \text{ mg}/\text{kg}$  ( $\sim 10\text{--}12 \text{ mg}$  assuming an average body weight of 75 kg) and single doses of 12 mg.



The finalised kinetic parameters describing ivermectin efflux were incorporated into the compound file as an  $CL_{intP-glycoprotein}$  of 2.5  $\mu\text{L}/\text{min}$  and a RAF of 0.1.

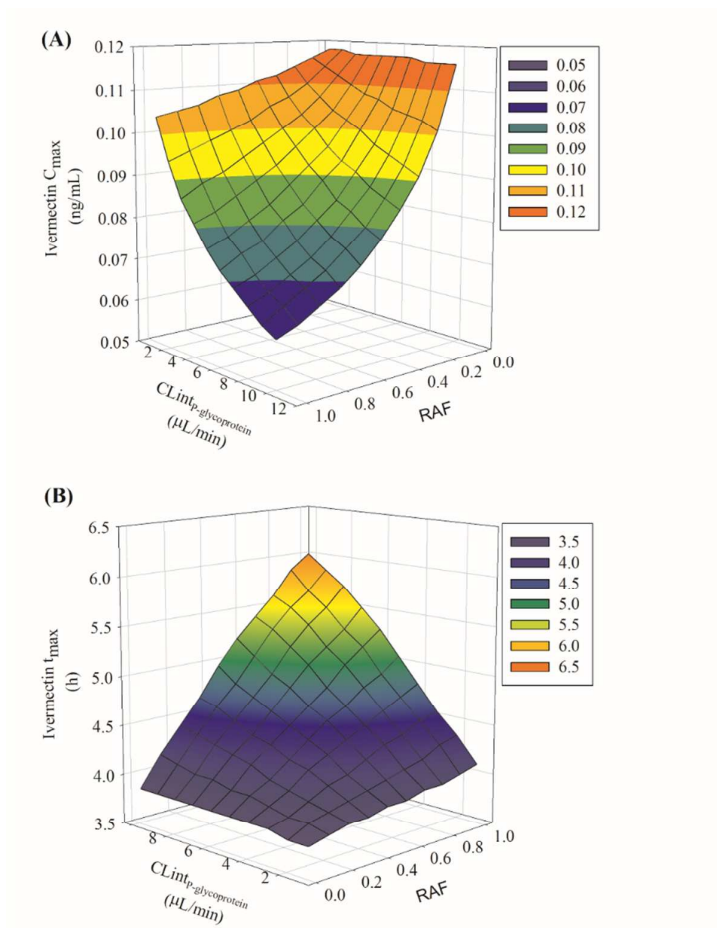


**Figure 1: Sensitivity analysis of active efflux and efflux scaling factor on ivermectin  $C_{max}$  and  $t_{max}$ .**

The sensitivity of P-glycoprotein active efflux clearance ( $CL_{intP-glycoprotein}$ ) and relative activity factor (RAF) on simulated ivermectin  $C_{max}$  (A) or  $t_{max}$  (B). A 60 mg oral dose was administered to a single healthy subject and the sensitivity of  $CL_{intP-glycoprotein}$  (1-10  $\mu\text{L}/\text{min}$ ) and RAF (0.10-1)  $C_{max}$  (A) or  $t_{max}$  (B) simulated over 100 simulations.

### *Solubility*

All dosing was conducted using a solid immediate release dosage form, with dissolution controlled by the intrinsic aqueous solubility with a Simcyp estimate of 0.0013 mg/mL

(estimate in literature: < 0.005 mg/mL <sup>13</sup>) assuming a melting point of 155 °C and using an empirical predictor equation developed by Jain and Yalkowsky <sup>14</sup>.

**Section 2: Thailand population group**

The age-weight distribution for male and female Thailand adult and paediatric subjects were extracted from age-weight distribution profiles developed by Hayes *et al* (2015) <sup>15</sup> and polynomial/linear equations applied to describe the shape of profiles using an approach described and implemented previously by our group <sup>16</sup>.

The resultant mathematical expression of age-weight distribution are detailed below:

*Adult Males*

$$\text{Weight} = 33.46 + (-0.3569*\text{age}^2) + (0.001522*\text{age}^4) / (1 + (-0.00755*\text{age}^2) + (2.78 \times 10^{-5}*\text{age}^4) + (-1.07 \times 10^{-9}*\text{age}^6))$$

*Paediatric Males*

$$\text{Weight} = 5.0164 + (1.74*\text{age})$$

*Adult Females*

$$\text{Weight} = -920.66 + (-188.63*\text{age}) + (22.48*\text{age}^{1.5}) + (-0.999*\text{age}^2) + (700.23*\text{age}^{0.5})$$

*Paediatric Females*

$$\text{Weight} = (5.635 + 1.121 * \text{age}) / (1 + -0.0282*\text{age})$$

For paediatric population groups, the age-weight relationship was calculated from 2-6 years of age. In the absence of appropriate age-height distributions, the relationship was assumed to be similar to that described by Simcyp for a healthy volunteer population group.

Blood biochemistry alterations (haematocrit and serum proteins) were also incorporated into the Thailand population group as described previously by our group <sup>16</sup>.

**REFERENCES**

1. Zeng Z, Andrew NW, Arison BH, Luffer-Atlas D, Wang RW 1998. Identification of cytochrome P4503A4 as the major enzyme responsible for the metabolism of ivermectin by human liver microsomes. *Xenobiotica; the fate of foreign compounds in biological systems* 28(3):313-321.

2. Long Q-C, Ren B, Li S-X 2001. Human pharmacokinetics of orally taking ivermectin. CHINESE JOURNAL OF CLINICAL PHARMACOLOGY 17(3):203-206.
3. Vanapalli S, Chen Y, Ellingrod V, Kitzman D, Lee Y, Hohl R, Fleckenstein L 2003. Orange juice decreases the oral bioavailability of ivermectin in healthy volunteers. Clinical Pharmacology & Therapeutics 73(2).
4. Takano R, Sugano K, Higashida A, Hayashi Y, Machida M, Aso Y, Yamashita S 2006. Oral Absorption of Poorly Water-Soluble Drugs: Computer Simulation of Fraction Absorbed in Humans from a Miniscale Dissolution Test. Pharmaceutical Research 23(6):1144-1156.
5. Canga AG, Prieto AMS, Liébana MJD, Martínez NF, Vega MS, Vieitez JJG 2008. The pharmacokinetics and interactions of ivermectin in humans—a mini-review. The AAPS journal 10(1):42-46.
6. Kigen G, Edwards G 2017. Drug-transporter mediated interactions between anthelmintic and antiretroviral drugs across the Caco-2 cell monolayers. BMC Pharmacology and Toxicology 18(1):20.
7. Krishna DR, Klotz U 1993. Determination of ivermectin in human plasma by high-performance liquid chromatography. Arzneimittel-Forschung 43(5):609-611.
8. Edwards G, Dingsdale A, Helsby N, Orme ML, Breckenridge AM 1988. The relative systemic availability of ivermectin after administration as capsule, tablet, and oral solution. European journal of clinical pharmacology 35(6):681-684.
9. Schinkel AH, Wagenaar E, van Deemter L, Mol CA, Borst P 1995. Absence of the *mdr1a* P-Glycoprotein in mice affects tissue distribution and pharmacokinetics of dexamethasone, digoxin, and cyclosporin A. Journal of Clinical Investigation 96(4):1698-1705.
10. Zhou D, Bui K, Sostek M, Al-Huniti N 2016. Simulation and Prediction of the Drug-Drug Interaction Potential of Naloxegol by Physiologically Based Pharmacokinetic Modeling. CPT: Pharmacometrics & Systems Pharmacology 5(5):250-257.
11. Troutman MD, Thakker DR 2003. Efflux ratio cannot assess P-glycoprotein-mediated attenuation of absorptive transport: asymmetric effect of P-glycoprotein on absorptive and secretory transport across Caco-2 cell monolayers. Pharm Res 20(8):1200-1209.
12. Guzzo CA, Furtek CI, Porras AG, Chen C, Tipping R, Clineschmidt CM, Sciberras DG, Hsieh JY, Lasseter KC 2002. Safety, tolerability, and pharmacokinetics of escalating high doses of ivermectin in healthy adult subjects. Journal of clinical pharmacology 42(10):1122-1133.
13. Williams JB, Nesbitt RU. 1989. Non-aqueous ivermectin formulation with improved antiparasitic activity. ed.: Google Patents.
14. Jain N, Yalkowsky SH 2001. Estimation of the aqueous solubility I: application to organic nonelectrolytes. Journal of pharmaceutical sciences 90(2):234-252.
15. Hayes DJ, van Buuren S, ter Kuile FO, Stasinopoulos DM, Rigby RA, Terlouw DJ 2015. Developing regional weight-for-age growth references for malaria-endemic countries to optimize age-based dosing of antimalarials. Bulletin of the World Health Organization 93(2):74-83.
16. Olafuyi O, Coleman M, Badhan RKS 2017. The application of physiologically based pharmacokinetic modelling to assess the impact of antiretroviral-mediated drug-drug interactions on piperazine antimalarial therapy during pregnancy.